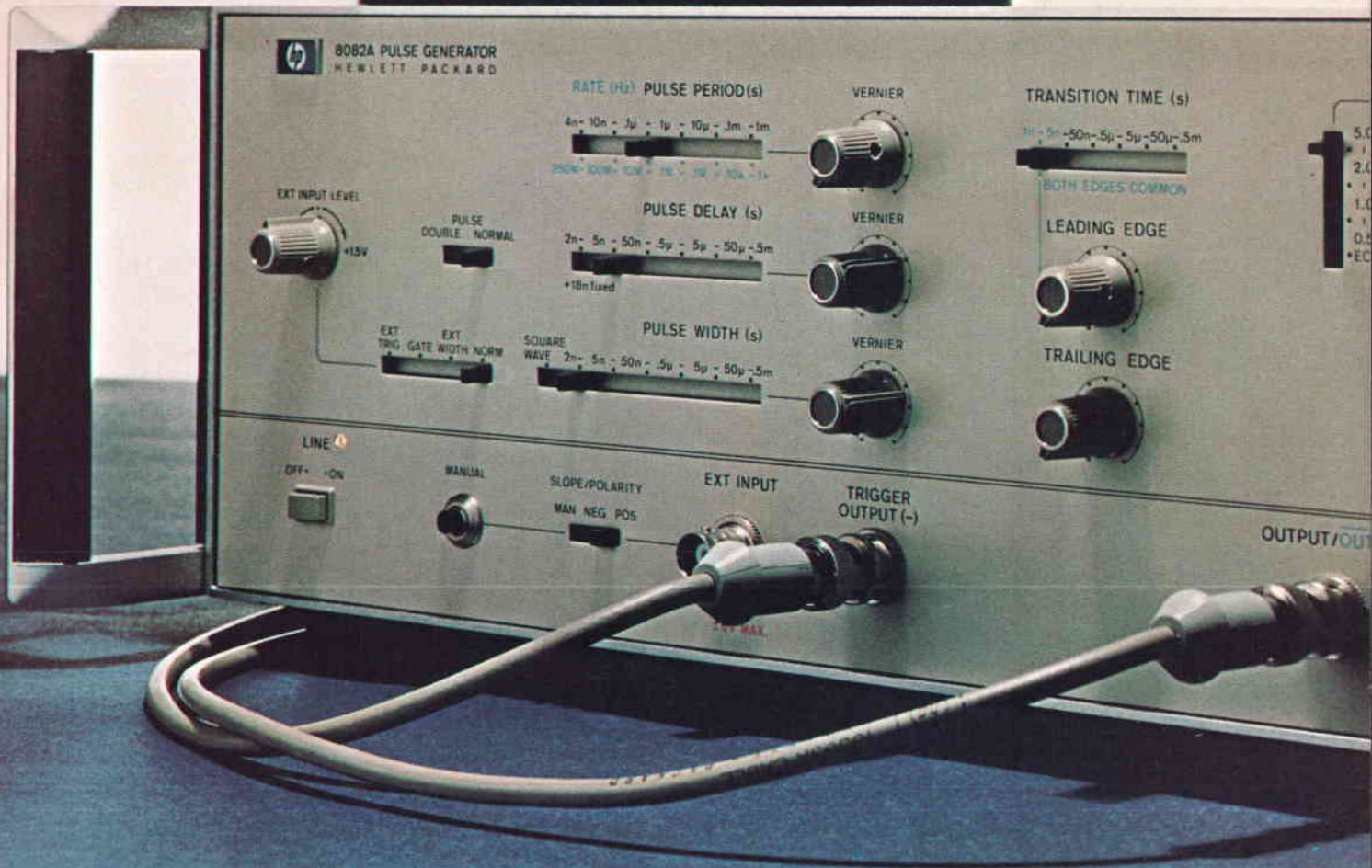
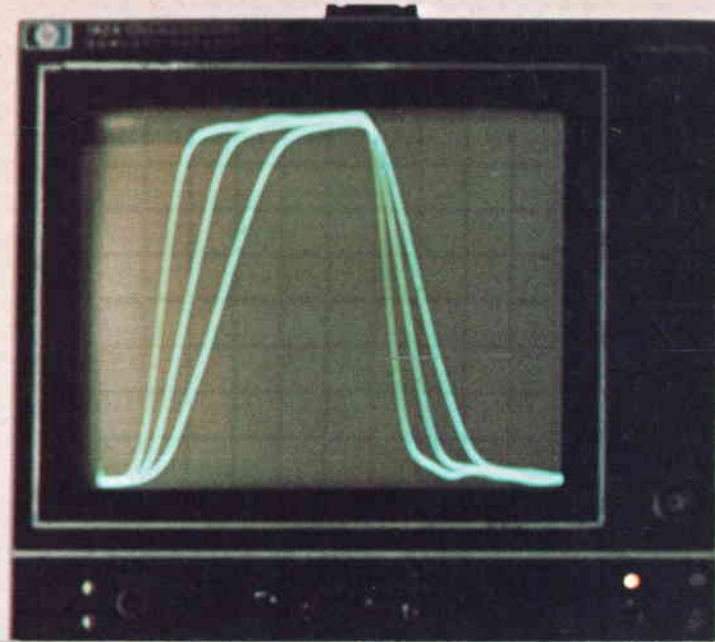


# HEWLETT-PACKARD JOURNAL



# A 250-MHz Pulse Generator with Transition Times Variable to Less than 1 ns

*Generating pulses at a 250-MHz repetition rate while giving the operator full control over the shape of these pulses requires microcircuit techniques.*

by Gert Globas, Joel Zellmer, and Eldon Cornish

**B**ECAUSE OF THE FLEXIBILITY that a general-purpose test instrument needs, designing such an instrument for testing advanced circuits poses a number of special problems. If it is to be useful, the instrument ought to be more versatile than the device it tests, and that is no simple matter when the devices' performance approaches the state of the art.

In response to the need for instruments capable of testing high-speed logic circuits such as ECL and Schottky-TTL, we started on the design of a pulse generator that would generate 5-volt pulses at repetition rates up to 250 MHz. Most importantly, this instrument would have pulse transition times variable down to less than 1 ns. Very fast transitions are needed for testing high-speed circuits but transitions that are too fast can cause problems of their own because they may become coupled into adjacent circuits. Variable transition times therefore were considered necessary for this instrument so designers could match pulse transition times to those found in their circuits.

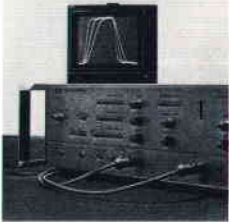
Developing circuits that would make transition times controllable down to 1 ns without causing excessive ringing or overshoot turned out to be the most challenging part of the project.

## A High-Speed Generator

The result of this design effort is shown in Fig. 1. This instrument, the Model 8082A Pulse Generator, produces pulses in a range of 0.5 to 5V at repetition rates up to 250 MHz. Pulse width is variable from 2 ns to 5 ms with transition times controllable from 5 ms all the way down to less than 1 ns.

Even so, the new pulse generator has the flexibility of a general-purpose instrument. It can operate with its own internal rate generator or in response to external triggers or a front-panel pushbutton. It supplies triggers for external equipment in syn-

chronism with the main pulse output with controllable delay between the trigger and main pulses. It has a double pulse mode that generates pairs of pulses for each rate trigger (up to 125 MHz) with as little as 2ns spacing between pulses, useful for checking the resolution capabilities of counting circuits. It can also operate in a squarewave mode at repetition rates up to 250 MHz, a handy way to check toggling rates. It has a gated mode for generating pulse bursts and it



**Cover:** *The Model 8082A Pulse Generator's output for three different transition-time settings is shown on the sampling oscilloscope display in this triple-exposure photograph. The oscilloscope sweep time is 1 ns/div, demonstrating that transition time is controllable down to 1 ns.*

**In this Issue:**  
A 250-MHz Pulse Generator with Transition Times Variable to Less than 1 ns, by Gert Globas, Joel Zellmer, and Eldon Cornish ..... **page 2**  
Optimizing the Design of a High-Performance Oscilloscope, by P. Kent Hardage, S. Raymond Kushnir, and Thomas J. Zamborelli ..... **page 8**  
A Thin-Film/Semiconductor Thermocouple for Microwave Power Measurements, by Weldon H. Jackson ... **page 16**  
Microelectronics Enhances Thermocouple Power Measurements, by John Lamy ..... **page 19**



**Fig. 1.** Model 8082A Pulse Generator gives control of transition times over a range of 1 ns to 5 ms and pulse repetition rates as high as 250 MHz. Two outputs are provided, one the complement of the other. To speed operator familiarization, the slide switches concerned with time functions are arranged horizontally while those concerned with pulse amplitude are arranged vertically.

can function as a pulse shaper to control the amplitude and transition times of pulses applied to the input.

The instrument has two outputs, one the complement of the other, to make it possible to drive complementary inputs and differential amplifiers. Amplitudes are separately controllable in steps. Both outputs are referenced to ground but may be offset  $\pm 2V$  (simultaneously) if the load requires bias as well as pulses. The AMPLITUDE selector also has an "ECL" position which automatically selects the amplitude and offset needed for ECL circuits. This fixes the baseline at  $-1.7V$  and the pulse top at  $-0.9V$  (into  $50\Omega$ ).

Of particular importance to those working with very fast circuits, the new pulse generator presents a well-matched source impedance to external  $50\Omega$  circuits (less than 2% reflection with pulse amplitudes up to  $4V$ ). Although the importance of a well-matched source impedance in pulse generators has been stressed for well over a decade, this importance is not diminished now that circuit dimensions are scaled down to microdimensions. The few picofarads of capacitance added by just a single gate or the few nanohenries of inductance of a bonding wire degrade a  $50\Omega$  termination sufficiently to cause noticeable reflection of very fast transitions, sometimes in an unpredictable manner such as that caused by the varying input impedance of a transistor during switching. Unless absorbed by the source, reflections could degrade the pulse shape significantly, giving misleading measurement results.

### Design Approach

In approaching the design of this instrument, it was recognized that to reduce performance-inhibiting stray capacitance and inductance to the barest minimum, monolithic integrated circuits would have to be used. IC's, manufactured by HP's Santa Clara Division, were developed specifically for this instrument.

Generating 5-volt pulses for 50-ohm circuits re-

quires appreciable current, with consequent heat. Heat removal is aided by bonding the high-power IC chips to hybrid microcircuit substrates. Thick-film hybrids are used because they enable a wider range of resistance values to be obtained.

The output amplifier requires a substrate with better heat conductance than the commonly-used alumina so a beryllium-oxide substrate, which has heat conductance comparable to that of brass, is used.

Even hybrid microcircuits have their limitations. Because nanosecond risetimes "see" an appreciable impedance in the tiny inductance of a bonding wire, the circuits were designed so that wherever possible waveform generation would involve the switching of current paths on the chip, with no abrupt changes in total chip current.

A block diagram of the new instrument is shown in Fig. 2. As can be seen it largely follows standard pulse generator practice in that the rate generator is followed by a delay generator, a pulse width generator, a transition-time generator, and an output stage.

### The Rate Generator

The pulse repetition rate is determined internally by the time it takes to charge a capacitor to a predetermined level, as has been common practice in recent pulse generators. But, to make it possible to generate square waves up to the maximum repetition rate, the Model 8082A discharges the capacitor at the same rate that was used for charging. The capacitor voltage waveform is thus triangular in shape, rather than a sawtooth as in earlier instruments, and the charge-discharge switch circuit generates square waves.

Model 8082A's rate generator is diagrammed in Fig. 3. Capacitor C1 is charged by constant current  $I+$  and discharged by  $I-$ , with switching controlled by emitter-coupled flip-flop Q2-Q3. During the charge phase, all of current  $I+$  is directed into capacitor C1, as shown by the arrows. This occurs when the emitter of Q1 is driven high, back biasing diode

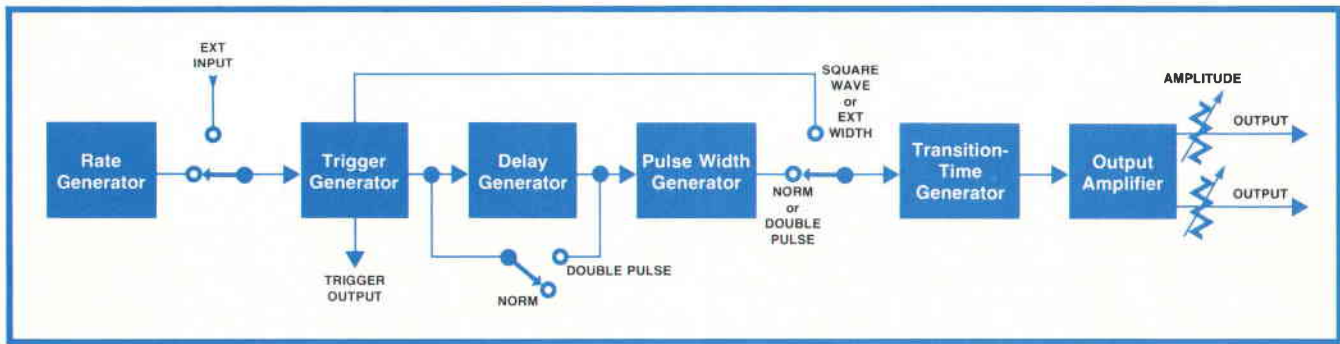


**Fig. 2.** Block diagram of the Model 8082A Pulse Generator. The basic arrangement is similar to other pulse generators in the HP 8000 series.

D1 and back biasing D4 by way of D3. At this time current  $I^-$  flows through diode D3 and transistor Q1.

When the voltage on capacitor C1 rises to the level that allows Q2 to conduct, regenerative action turns Q2 full on and turns off Q3. The drop at the collector of Q2 turns off Q1.

When Q1 goes off, the  $-10V$  supply pulls down on D1, back biasing diodes D2 and D3. Current  $I^-$  now discharges capacitor C1 while  $I^+$  flows to the  $-10V$  bus by way of diode D1.

The circuit remains in this state until the capacitor voltage falls to the point that allows Q3 to conduct, initiating regenerative action that turns Q2 off and Q3 full on to start a new cycle. The output, taken from the collector of Q3, is thus a square wave.

Transistor Q4 equalizes the current into the  $-10V$  bus by supplying a current equal to  $I^+$  when  $I^+$  is directed into C1.

The repetition rate range is changed by switching the value of capacitor C1 and vernier control is provided by adjusting the levels of  $I^+$  and  $I^-$ . On the fastest range, minimum capacitance is achieved by back-biasing diodes on the chip to decouple external connections.

The output of Q3 is passed on 50-ohm stripline to the trigger generator. This circuit, another monolithic IC, consists largely of gates for buffering the signal to the trigger output connector and for shaping the leading edge into a narrow pulse (2 ns) and its complement for driving the delay generator.

When the instrument is in the manual or external trigger mode or the external width mode, the rate generator is turned off. Manual or external triggers are applied by way of a trigger amplifier directly to the trigger generator.

### Delay and Width Generators

The delay circuit is an IC monostable multivibrator that is set by the trigger generator pulses. When set, it starts the charge of a capacitor and when the capacitor reaches a trigger level, the circuit resets. As in the rate generator, delay ranges are changed by

switching capacitors and vernier control is provided by the charging current level.

The pulse-width circuit IC is identical to the delay IC. It is set by the trailing edge of the delay generator pulse, and it resets itself when the width capacitor reaches the upper trigger level. When the instrument is set to the double-pulse mode, the trigger that starts the delay generator is also gated through to the width generator, so the width circuit generates two pulses for each rate generator pulse. This mode is useful for checking the ability of trigger circuits to respond to two closely-spaced pulses. Because of the presence of two pulses for each rate pulse, the maximum repe-

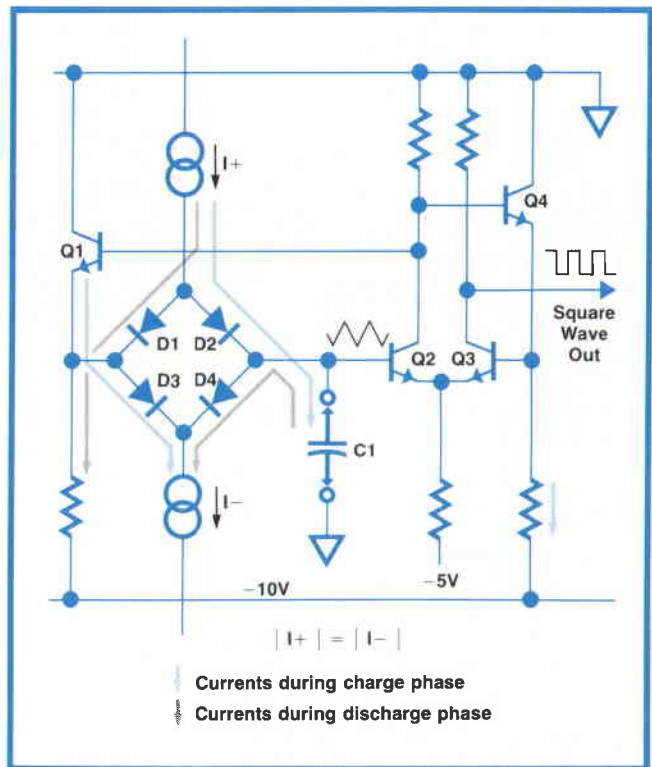


**Fig. 3.** Simplified diagram of the rate generator. Equal charge and discharge times of capacitor C1 result in a square wave output. Ranges are changed by switching capacitor C1; currents  $I^+$  and  $I^-$  provide vernier control of rate.

tion rate in this mode is limited to 125 MHz.

In the squarewave mode, the delay and width circuits are inhibited and the squarewave output of the rate generator is gated through the trigger generator directly to the transition-time generator. External waveforms follow the same path when the instrument is in the EXT WIDTH mode. In this case, the trigger generator is turned on and off by the external waveform rather than by the rate generator.

The output of the width generator is subjected to a dc translation in a level shifter (not shown in Fig. 2). This change of level is required because the circuits are dc coupled to preserve baseline stability, with the output stage driving a load resistor returned to ground level. To account for the voltage shifts engendered by the intervening circuits, the baseline level of the width generator output is shifted down to  $-19V$  by a bistable circuit. This circuit uses PNP transistors which, along with the use of zener diodes to absorb some of the voltage drop, made it difficult to incorporate into an integrated circuit (very fast integrated circuits use NPN transistors exclusively). Hence, discrete components are used here.

#### The Transition-Time Generator

Operation of the transition time generator basically is similar to that of other pulse generators: the rectangular input drives a switching circuit whose output can change states only as fast as a capacitor at its output can be charged. The capacitor is charged by a constant current so the slope of the resulting waveform is linear. The same is true of the capacitor discharge on the trailing edge of the pulse. Clamp circuits fix the upper and lower excursions of the capacitor voltage.

To permit very fast transition times at high repetition rates, the new pulse generator uses a "push-pull" arrangement, shown in simplified form in the diagram of Fig. 4. The two currents  $I_L$  and  $I_T$  represent the constant currents for generating the pulse leading edge ( $I_L$ ) and trailing edge ( $I_T$ ). To describe circuit operation, let us assume that the circuit is resting, so to speak, between pulses with Q13 turned on and Q14 off. The voltage on capacitor C11 is at the lower clamp voltage and the voltage on C12 is at the upper voltage. With Q14 off, current  $I_T$  passes through clamp diode D14 to the upper clamp voltage source and an equal amount flows from the lower clamp voltage source through diode D11 and thence through Q13, along with  $I_L$ .

Now, a pulse applied to transistors Q11 and Q12 turns off Q13 and turns on Q14. Current  $I_L$  is now diverted into C11 and it starts charging C11, which back-biases diode D11.

With Q14 turned on, current  $I_T$  now flows through Q14 but because the emitters of Q11 and Q12 are re-

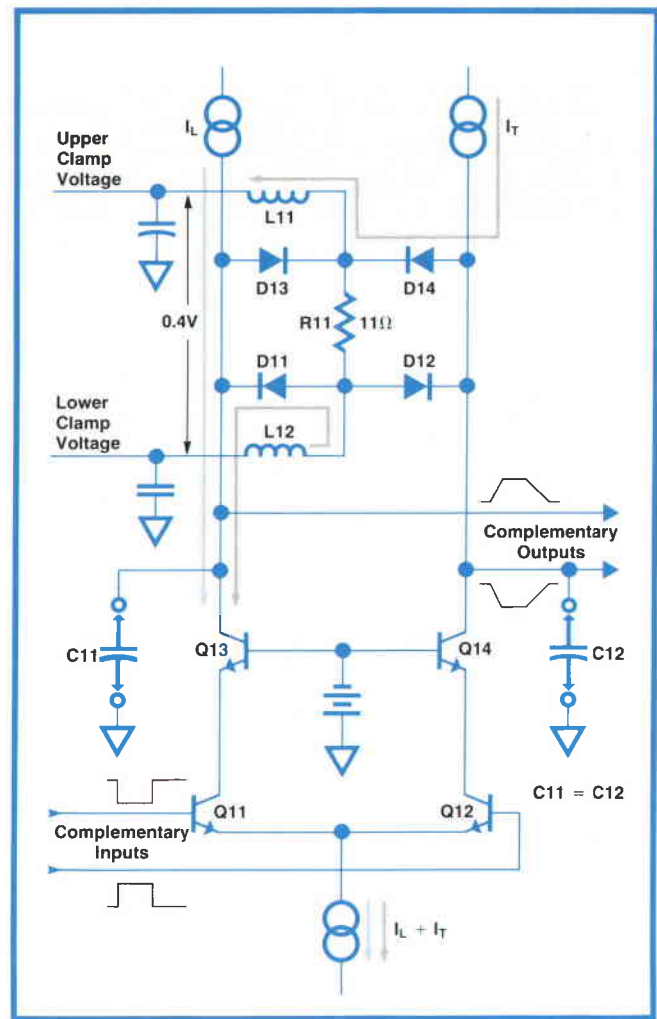


Fig. 4. Simplified diagram of the transition-time generator. Vernier control currents  $I_L$  and  $I_T$  are separately adjustable except on the fastest range.

turned to a current source, transistor Q14 is constrained to pass a current equal to  $I_L + I_T$ . Thus, until diodes D12 and D13 become forward biased, a portion of the total Q14 current equal to  $I_L$  is drawn from capacitor C12, discharging this capacitor. This action continues until C12 reaches the lower clamp level, which coincides with C11 reaching the upper clamp level (obviously, C11 and C12 must be closely matched in value). Current  $I_L$  then flows through diodes D12 and D13 to Q14 by way of the voltage clamps.

When the input pulse terminates, the reverse action occurs, but now the discharge current out of C11 and the charge current into C12 each equal  $I_T$ .

Transition times are determined by the values of the capacitors and the levels of the constant currents. On the very fastest range, it was found that a cleaner waveform resulted if the circuit were balanced with  $I_L$  and  $I_T$  made equal. On this range, then, vernier control is by one control that adjusts both current levels simultaneously.

Even with the microdimensions of integrated circuits, there was a problem with ringing in this circuit caused by parasitic reactances. The main contributors were the inductances L11 and L12 created by the bonding wires. Ringing was reduced by adding the damping resistor R11 and by using two bonding wires in parallel for each connection.

The outputs of the transition-time generator go to a differentially-driven impedance converter (not shown) that drives 2V into a 25Ω load. This circuit also has means for switching each of the push-pull signals into the opposite channel when it is desired to complement the outputs.

**Output Stage**

The output amplifier is a dual cascode circuit driving two complementary outputs. As can be seen in the diagram of Fig. 5, the circuit operates at below ground voltage levels so, to produce positive pulses with the baseline at ground level, dc offset currents are added automatically to the outputs such that the

baseline remains fixed at ground level. When the instrument is switched to operate in the negative pulse mode, these offset currents are switched off. Variable offset currents, giving the operator the option of placing the baseline anywhere in a range of ±2 V, are added following the attenuator.

The output stage actually consists of three amplifiers operating in parallel, all of the transistors being on one monolithic chip. In this way, small transistors, needed for wide bandwidth, can be used to obtain the 200 mA drive current needed to obtain 5 V across the internal 50 ohms and external 50 ohms in parallel.

The output transistors appear as a current source to an external load, so the instrument's source impedance is determined by the 50-ohm loads in the collector circuits.

The attenuator is switched in steps by miniature relays that introduce but a small amount of stray reactance, easily compensated for. Vernier control is performed electronically by transistors Q24 and Q25 in the amplifier (Fig. 5). The emitter of Q24, for ex-

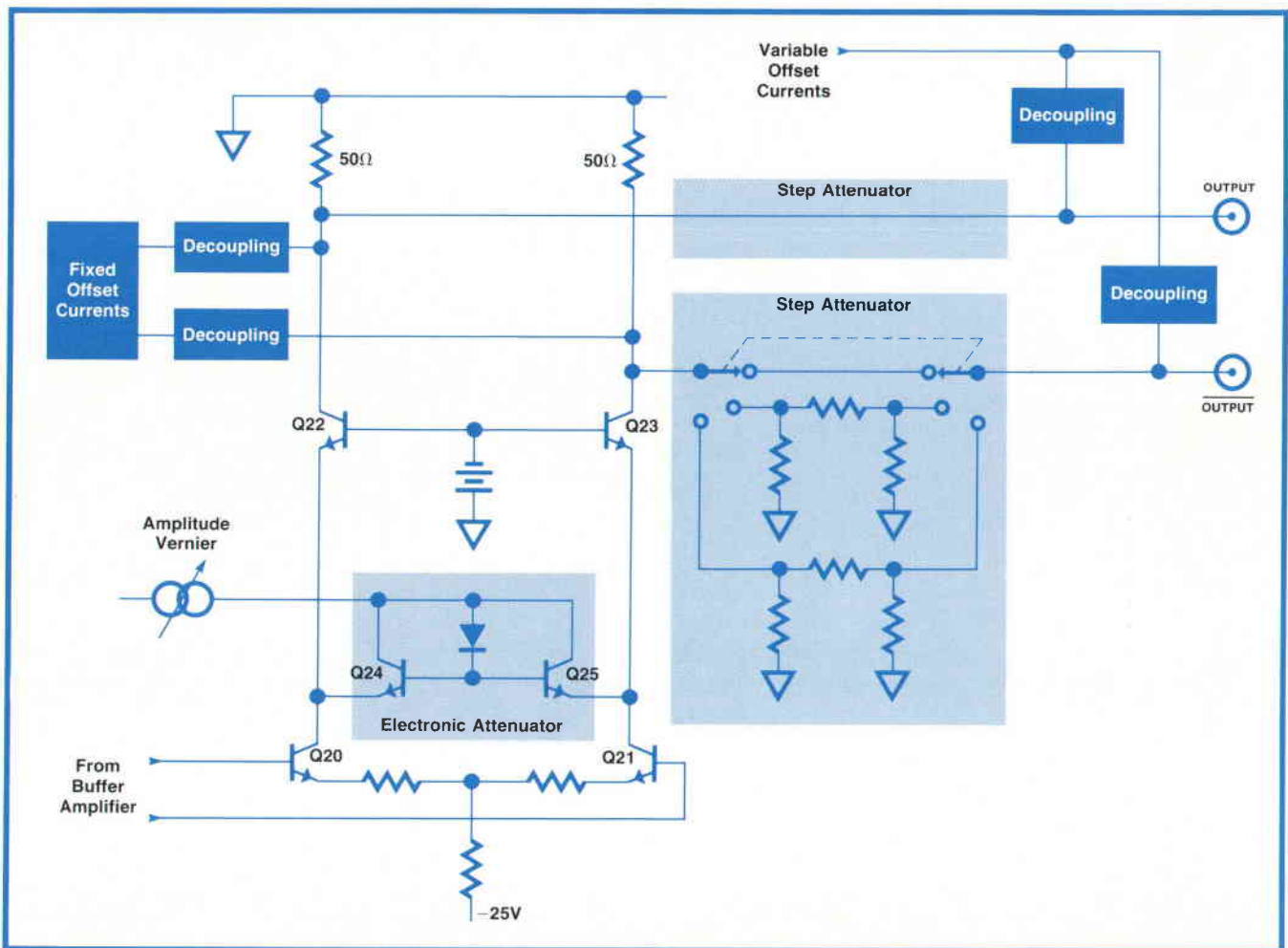


Fig. 5. Simplified diagram of the output stage. The amplifier functions as a current source, so source impedance is established by the 50Ω collector load resistors.

ample, is in parallel with the Q22 emitter so it withdraws some of the current passing through Q20, the amount withdrawn being determined by the AMPLITUDE VERNIER control.

When the front-panel AMPLITUDE controls are set to the ECL position, the appropriate attenuation level is set and a fixed offset current is substituted for the variable current.



## Acknowledgments

The 8082A Pulse Generator project originated in the HP Colorado Springs Division under the direction of James Umphrey, group leader, and it was completed at Hewlett-Packard GmbH under group leader Dieter Vogt. Besides the authors, Wolfgang Staudt contributed to the electrical design. Mechanical design was by Rainer Eckert. 

### Eldon Cornish

A 1959 graduate of the University of Nebraska (BS in Physics and Math), Eldon Cornish spent 9 years on the east coast in applied research, primarily in digital communications, then 18 months in IC circuit design in Texas and finally at HP Colorado Springs where he became involved in IC design for the 8082A Pulse Generator. Outside of working hours, Eldon likes to hike and ski, both touring and downhill, taking along the whole family (wife and 4 kids, 12, 10, 8 and 7). He also serves on various church boards and sings in the choir.

### Joel Zellmer (left)

Joining the Hewlett-Packard Colorado Springs Division in 1966, Joel Zellmer worked on the 220A/221A Squarewave Generators and the 1120A 500 MHz Probe before going on to IC development. He transferred to HP GmbH in April 1973. Joel is keen on sailing, skiing and constructing/piloting radio-controlled model gliders. He and his wife have one son, 4.

### Gert Globas (right)

Gert Globas graduated from the University of Stuttgart (Diplome-Ingenieur) in 1969 and then joined the acoustical instrumentation group at HP GmbH. Subsequently he became project leader on the 9104 and 9863 Calculator Tape Readers before taking on the 8082A project. Gert is president of the HP GmbH R and D soccer team and he also likes to ski. A once-upon-a-time piano-player Gert enjoys classical music and he dabbles in photography, both movie and still.

## SPECIFICATIONS

### Model 8082A Pulse Generator

#### Pulse Characteristics (50Ω source and load impedance)

**TRANSITION TIMES:**  $\leq 1\text{ns} - 0.5\text{ms}$  in 6 ranges. First range ( $< 1\text{ns}$  to  $5\text{ns}$ ) controls leading and trailing edges simultaneously. Transition times for all other ranges variable independently up to 1:10.

**OVERSHOOT AND RINGING:**  $\leq \pm 5\%$  of pulse amplitude; may increase to  $\pm 10\%$  with amplitude vernier CCW.

**PRESHOOT:**  $\leq \pm 5\%$  of pulse amplitude.

**LINEARITY:** Linearity aberration  $\leq 5\%$  for transition times  $> 5\text{ns}$ .

**OUTPUT:** Maximum pulse amplitude is 5V from 50Ω into 50Ω. Maximum output voltage (amplitude + offset) is  $\pm 5\text{V}$ .

**OFFSET:** + 2V into 50Ω.

**DC-SOURCE IMPEDANCE:** 50Ω  $\pm 5\%$ .

**REFLECTION COEFFICIENT:** Reflection is 2% typical for steps with 1ns rise time applied to output connector on all amplitude ranges except 5V range. Reflection may be up to 15% on 5V range.

**OUTPUT PROTECTION:** Cannot be damaged by open or short circuits or applications of ext  $\pm 6\text{V}$  or  $\pm 200\text{mA}$ , independent of control settings.

**ATTENUATOR:** Two separate three-step attenuators reduce outputs to 1V. Vernier is common for both outputs and reduces output to 0.4V minimum. Fourth attenuator position provides ECL-compatible outputs (typically  $-0.9\text{V}$  to  $-1.7\text{V}$  open circuit).

#### Timing

**REPETITION RATE:** 1 kHz to 250 MHz in 6 ranges.

**PERIOD JITTER:**  $< 0.1\%$  of setting + 50ps.

**DELAY:** 2ns - 0.5ms in 6 ranges plus 17ns typically with respect to trigger output.

**DELAY JITTER:**  $< 0.1\%$  of setting + 50ps.

**DOUBLE PULSE:** Up to 125 MHz max (simulates 250 MHz).

**DELAY DUTY CYCLE:**  $> 50\%$ .

**PULSE WIDTH:**  $< 2\text{ns} - 0.5\text{ms}$  in 6 ranges.

**WIDTH JITTER:**  $< 0.1\%$  of setting + 50ps.

**WIDTH DUTY CYCLE:**  $> 50\%$ .

**SQUARE WAVE:** Pulse Width switch has position that provides square wave output with max Rep Rate of 250 MHz (delay and double pulse are disabled). Duty cycle is  $50\% \pm 10\%$  up to 100 MHz,  $50\% \pm 15\%$  for  $> 100\text{MHz}$ .

**TRIGGER OUTPUT:** Negative-going square wave (50% duty cycle typ.)  $> 500\text{mV}$  from 50Ω into 50Ω. Internal 50Ω load can be switched off by slide-switch on PC-board, increasing amplitude to  $\geq 1\text{V}$  into 50Ω up to 200 MHz.

### Externally Controlled Operation

#### EXTERNAL INPUT

**INPUT IMPEDANCE:** 50Ω  $\pm 10\%$ , dc-coupled.

**TRIGGER LEVEL:** Adjustable  $-1.5\text{V}$  to  $+1.5\text{V}$ .

**SLOPE CONTROL:** Positive or negative. Manual position enables pushbutton to trigger single or double pulse generation, in EXT TRIG mode, or pulse burst in GATE mode (button pushed in simulates "on" signal).

**SENSITIVITY:** Sine-wave  $> 200\text{mV}$  pp, pulses  $> 200\text{mV}$ .

#### EXTERNALLY-CONTROLLED MODES

**EXT. TRIGGER:** Rep rate is externally controlled; approximately 7ns delay between external input trigger and trigger output. Square-wave mode is disabled.

**SYNCHRONOUS GATING:** Gating signal turns rep rate generator on. Last pulse is normal width even if gate ends during pulse.

**EXTERNAL WIDTH:** Output pulse width determined by width of external input waveform, Rep rate and delay are disabled. Trigger output provides shaped input signals.

### General

**POWER REQUIREMENTS:** 100V, 120V, 220V, 240V (+5%, -10%) 48-440 Hz, Power consumption 85VA max.

**WEIGHT:** Net 17½ lbs (7.9 kg).

**DIMENSIONS:** 16-3/4 in wide  $\times$  5-11/16 in  $\times$  15 in deep (426  $\times$  145  $\times$  380 mm).

**PRICE IN U.S.A.:** \$3355.

**MANUFACTURING DIVISION:** Hewlett-Packard GmbH  
Herrenberger Strasse 110  
D-7030 Böblingen, Württemberg  
Germany

# Optimizing the Design of a High-Performance Oscilloscope

*A wideband oscilloscope is more useful if its performance is not subject to variations that may degrade measurement accuracy. Its value is even more apparent if this consistent performance is achieved at moderate cost, both initial and long-term.*

by P. Kent Hardage, S. Raymond Kushnir, and Thomas J. Zamborelli

**A**LTHOUGH BANDWIDTH IS THE specification most often referred to in evaluating a high-performance oscilloscope, users regard rise time (0.35/bandwidth) as a more meaningful indicator of a scope's usefulness. Designers of fast switching circuits who wish to measure switching time, propagation delay, and so on, or designers of wideband analog circuits who wish to measure transient response, all need to understand the rise time capabilities of the oscilloscopes they use.

Obtaining fast rise time requires sophisticated design techniques that can be very expensive unless trade-offs or compromises are made—compromises

that may be counterproductive. For example, if many adjustments are needed to "tweak up" the scope to get high performance, not only will the initial cost become higher because of the extra time needed in production, but long-term maintenance costs will also be higher.

Achieving an optimum balance of characteristics at an affordable price thus became the major design goal for the new Hewlett-Packard 275-MHz Model 1720A Dual-Channel Oscilloscope (Fig. 1). As a result of this effort, the 1.3-ns rise time of this instrument is maintained at all settings of the step and variable attenuators and in either the 50 $\Omega$  or high-imped-

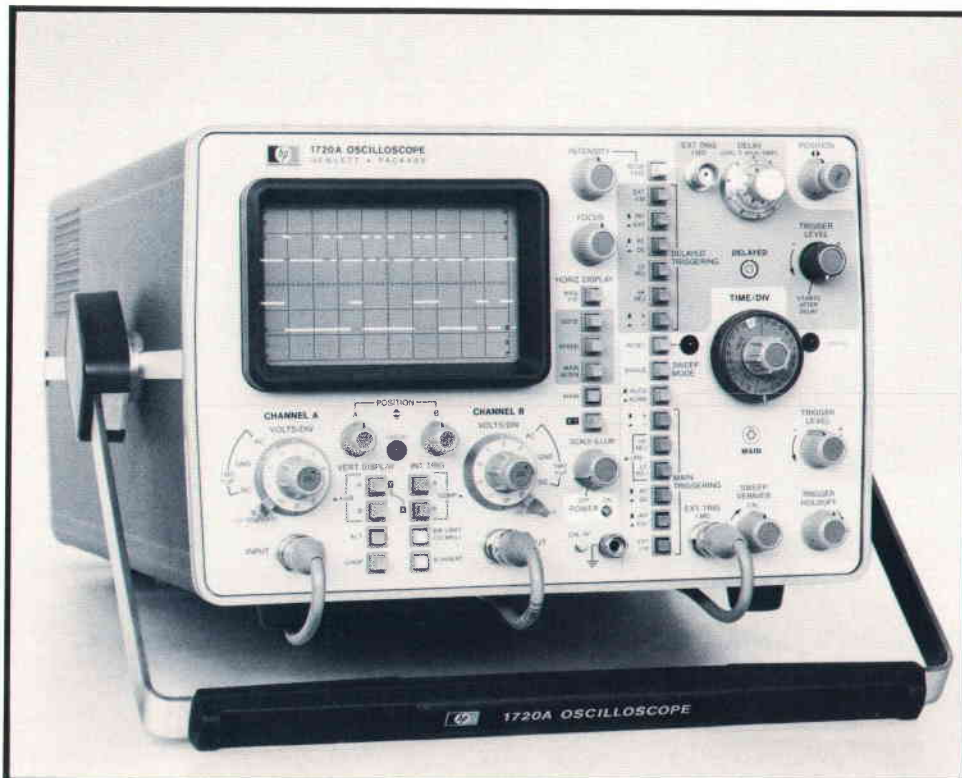


**Fig. 1.** Model 1720A Oscilloscope has dc-275 MHz bandwidth, delayed sweep, and all the other attributes of a general-purpose, laboratory-grade oscilloscope. Operating modes are easily selected by color-coded pushbuttons that are in clearly defined relationships (blue for display, green for trigger operation, and so on), reducing familiarization time.

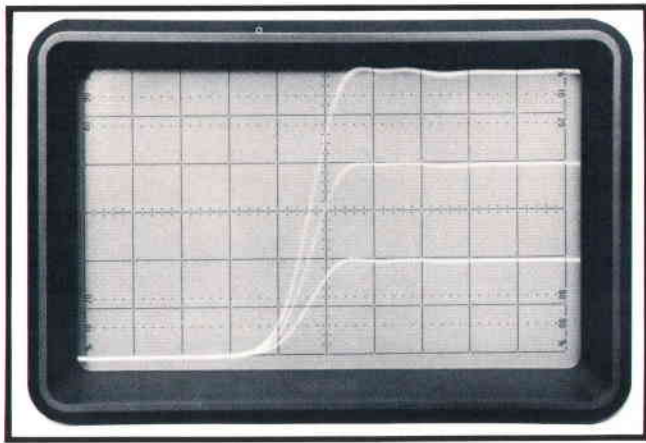


**Fig. 2.** Multiple exposure oscillogram displays the same input voltage step at three different amplitude vernier settings, showing that use of the vernier does not degrade rise time nor does it affect the baseline (sweep time is 1 ns/cm).

ance input modes. This consistency of performance (Fig. 2) is needed by those concerned with measuring rise times, since adjusting the waveform to exactly the vertical deflection needed for a rise time measurement invariably requires use of both the step and variable attenuators.

What is more, the consistent performance is maintained over a 0-to-55°C temperature range. Although it is not expected that the new oscilloscope will be used in extreme environments, it often happens that it becomes warmed or chilled while in transit, so the wide temperature specification assures that measurements can be made accurately as soon as the user arrives at his destination.

Commensurate with the consistent rise time, sweep times were designed to maintain accuracy and linearity of  $\pm 3\%$  or better over the 0-to-55°C temperature range and over the full 10-cm display width. Time interval measurements using the delayed sweep to successively position the two points of interest at center screen can be made with 1% accuracy.

#### Designed-in Reliability

Another important aspect of oscilloscope design concerns maintainability. It is not widely appreciated that much of the total cost of an instrument's ownership can be involved in maintenance. For this reason, the number of internal adjustments within the Model 1720A was held to 56, about half that of comparable instruments. The time required by the calibration lab is thus reduced significantly. Furthermore, the mechanical design was made as open as possible, as shown in Fig. 3, to make the adjustments readily accessible.

In addition to the designed-in long-term reliability evidenced by the wide operating temperature range, maintenance problems are reduced by subjecting

every 1720A Oscilloscope to a heat cycling test to weed out any unstable components. Every Model 1720A is also subjected to a shake table test to assure that there are no poor connections or loose hardware.

#### Premium Performance

Basically, the Model 1720A was designed to have all the performance characteristics of a high-quality lab oscilloscope, such as wide bandwidth, fast sweeps, 2% attenuator accuracy, delayed sweep, and so on. It is packaged, however, in the compact 1700-series cabinet for both bench-top and portable convenience.

The vertical deflection factor ranges from 10 mV/div to 5V/div (to 12.5 V/div with the vernier control). The input has switchable input impedance, either a well-matched 50Ω (VSWR less than 1.3:1) or one megohm shunted by an exceptionally low 11 pF. Sweep times range from 10 ns/div to 0.5s/div (to 1.25s/div with the vernier). The fastest sweep (main or delayed) can be extended to 1ns/div with the  $\times 10$  sweep magnifier.

Triggering is notably stable, requiring only 1 cm deflection of signals up to 300 MHz for both the main and/or the delayed sweep (trigger selection, as well as other modes of operation, are described in detail on page 15).

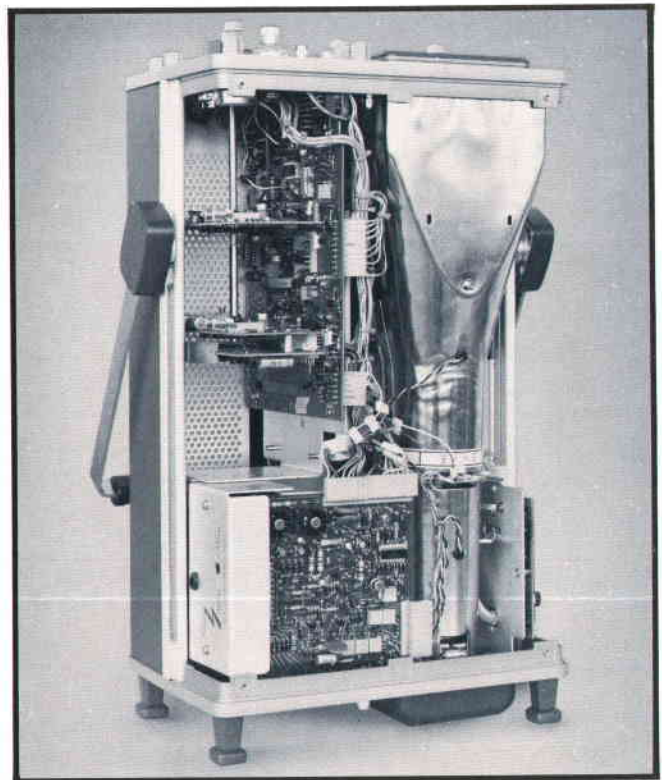


**Fig. 3.** Cabinet covers lift off for easy access to the interior for calibration and servicing. All adjustments are directly accessible with the covers removed.

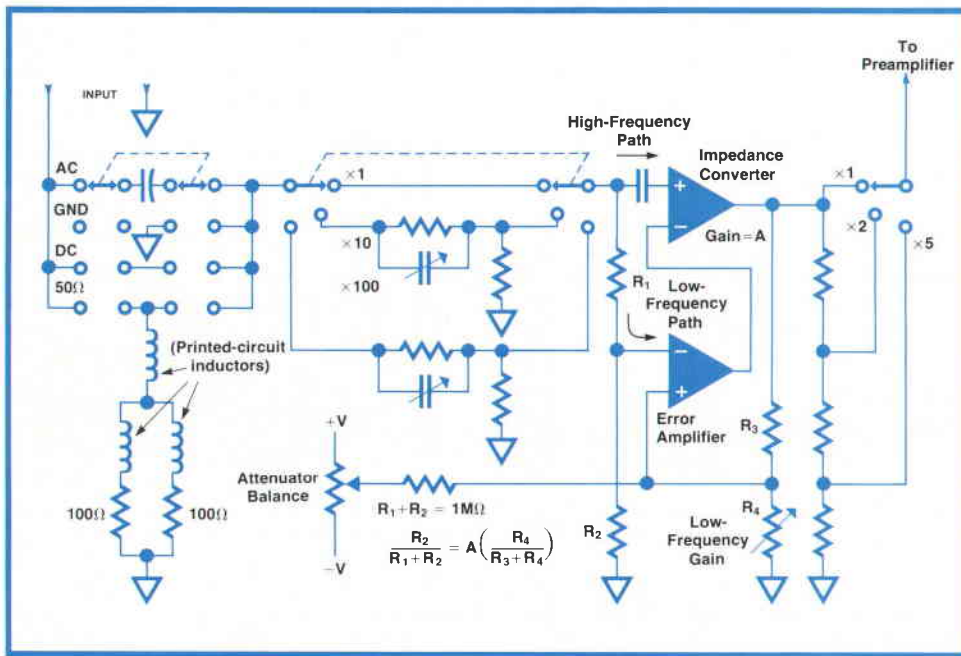


**Fig. 4.** Simplified schematic of the vertical input attenuator. Repeatable performance is obtained by mounting the discrete components that form the attenuator on a printed-circuit board. The parallel 100Ω resistors for the 50Ω termination are mounted in plug-in sockets for easy replacement whenever excess input voltage (>10V) may cause them to burn out.

### Well Integrated

A key factor in obtaining the stable high performance of this oscilloscope at moderate cost is the high level of circuit integration made possible by present-day solid-state monolithic technology. The circuits that evolved are perhaps the most complex high-frequency monolithic integrated circuits ever developed (30-40 2-GHz transistors per chip). As a consequence, the wide bandwidth performance was achieved with a lower component count, with fewer calibration adjustments, and with reduced printed-circuit board complexity.

Also contributing to the high performance is a helical-electrode CRT deflection system, similar to that used in the Model 183A Oscilloscope,<sup>1</sup> and a new attenuator design that gives full bandwidth with a high-impedance input, as well as a 50Ω input.

### Full Bandwidth Attenuator

The attenuator configuration is diagrammed in Fig. 4. As has often been done, the design splits the attenuator into two sections with an impedance converter between. This new version eliminates shifts in baseline as the range is changed, a consequence of dc offsets from drift in the impedance converter.

Both stable, ground-level output and high-frequency performance were obtained by the two-path impedance converter shown in Fig. 4. The high-frequency path is through an ac-coupled FET source-follower that drives an emitter-follower. The low-frequency path is through the error amplifier (the crossover frequency is about 1 kHz). Because the error amplifier is a stable operational amplifier, there is no dc translation of baseline through the impedance-con-

verter, and thus no shift in a zero-level baseline when the attenuator is switched. This performance is achieved without a differential amplifier using expensive, high-frequency dual FET's.

The first section of the attenuator contains only the ×1, ×10, and ×100 sections. The attenuator sections are switched on the circuit board by spring fingers actuated by cams on the switch shaft (see Fig. 5). This switching arrangement shortens signal paths, reduc-

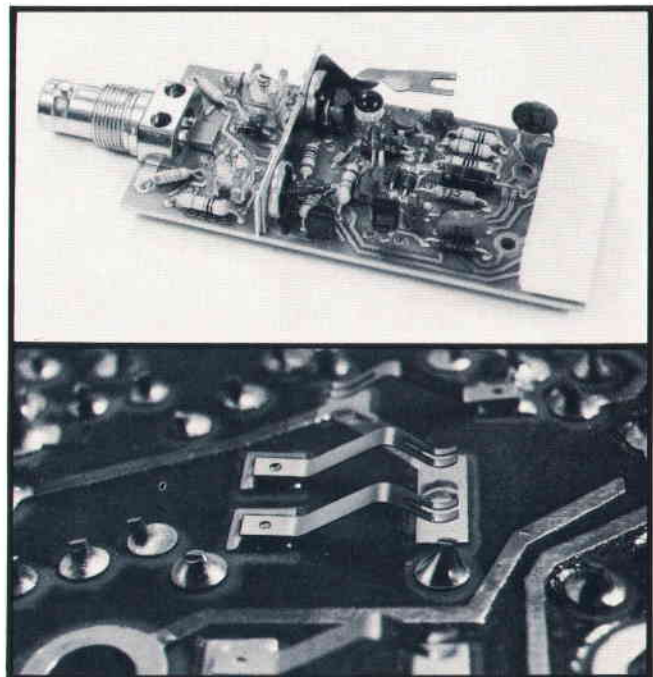


**Fig. 5.** Attenuator components are mounted on a circuit board. Close-up view shows the spring-finger contacts that switch the attenuator on the back side of the board.

ing parasitic capacitance and inductance.

Since the  $\times 1$  position is essentially a straight-through connection, the remaining two attenuator sections can be physically located on either side of the straight-through path, giving a repeatable, symmetrical configuration that does not require padding capacitors to equalize the stray capacitance of the attenuator sections. Only one trimming capacitance per section is thus required.

The "in-between" attenuator steps ( $\times 2$ ,  $\times 5$ ) are obtained in the second attenuator. Since this is driven by the impedance converter, it can be a low-impedance ( $200\Omega$ ) attenuator that uses fixed capacitive compensation. Thus, the entire attenuator has only two trimming adjustments.

This design gives full-bandwidth performance, and it has an exceptionally low input capacitance (11 pF). Hence this same attenuator is used when the input is switched for  $50\Omega$  input impedance. A good match to 50 ohms is achieved by switching in a compensated  $50\Omega$  shunt termination at the input.

### Organizing the Vertical Channels

A major problem in the design of a high-frequency oscilloscope is the manner of connecting the front-panel controls to the circuits they control. This led to the use of parallel common-base stages in the vertical channel preamplifier with dc voltages controlling which transistors of each pair will pass or block the signal.

The sequence of controls is diagrammed in Fig. 6. In a departure from traditional design, the sync pick-off occurs ahead of the other control functions, rather than further down the chain as has been common practice. With this arrangement, changing the position, polarity, or amplitude vernier controls does not cause a loss of sync since these controls have no effect on the point on the waveform where triggering occurs. This contributes to operator ease in maintaining a triggered display. The trade-off is that the sync amplifier requires a wide dynamic range so that no part of the waveform that can be brought on screen with the position control will lie in the cut-off or saturation region of the sync amp.

The final stages of the preamps in both channels drive a common load. Control currents to the final stages, the ON-OFF switches, determine the mode of operation, e.g., either channel alone, both channels in an  $A + B$  or  $A - B$  mode, both channels alternately per sweep or chopped at a 1-MHz rate.

The circuits for the functions diagrammed in Fig. 6 are in a differential cascode configuration using 35 2-GHz transistors. These are all contained in one  $43 \times 46$  mil chip. The two chips for the two vertical channels are mounted on one alumina substrate that includes 16 laser-trimmed thick-film resistors and

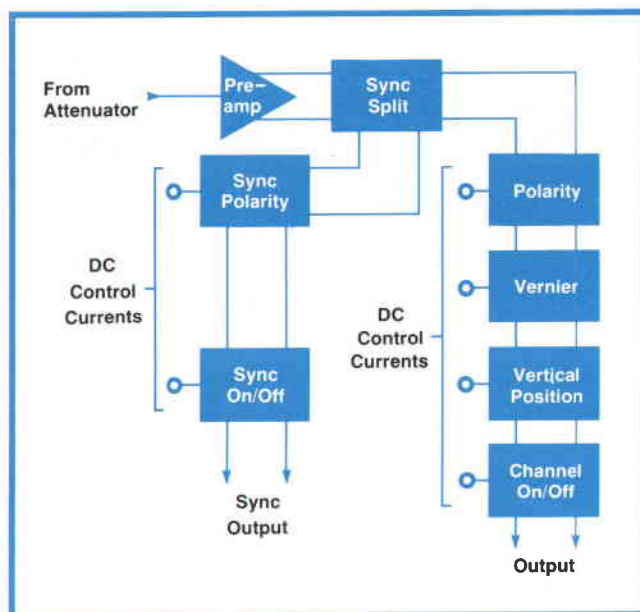


**Fig. 6.** Block diagram of the vertical channel preamplifier. DC control currents bias parallel-connected transistors individually to select the signal path.

40 contact pads. The pads make contact to spring fingers on the printed-circuit board. None of the connections are soldered so removal of this circuit for trouble-shooting or replacement requires only the removal of the four screws that retain the plastic holder (Fig. 7).

### CRT Drive

The combined output of the preamplifiers goes through a 50-ns delay line and then to the output amplifier. The output amplifier has two IC's, one in a 16-lead DIP and one on an alumina substrate that also has 6 thick-film resistors for biasing. This arrangement minimizes parasitic capacitance and inductance while giving precise control of those that remain.

The output stage is a "sliding cascode" stage like that used in the Model 1830A Vertical Amplifier<sup>2</sup> for the Model 183A Oscilloscope. Because of the high power requirements, special care was taken to keep current densities in the metalization on the IC chip to less than  $5 \times 10^5$  A/cm<sup>2</sup>. The design also keeps the worst-case junction temperature to less than 125°C.

The substrate is epoxied to an aluminum holder that in turn is clamped to an aluminum heat sink that conducts the heat to a radiator on the rear panel. A fan is not required to keep internal heat rise low.

Electrical connection from the alumina substrate to the printed circuit board is by way of the same kind of no-solder, spring-finger contact used for the preamplifier.

### Time Base

Both sweep generators (main and delayed) use the

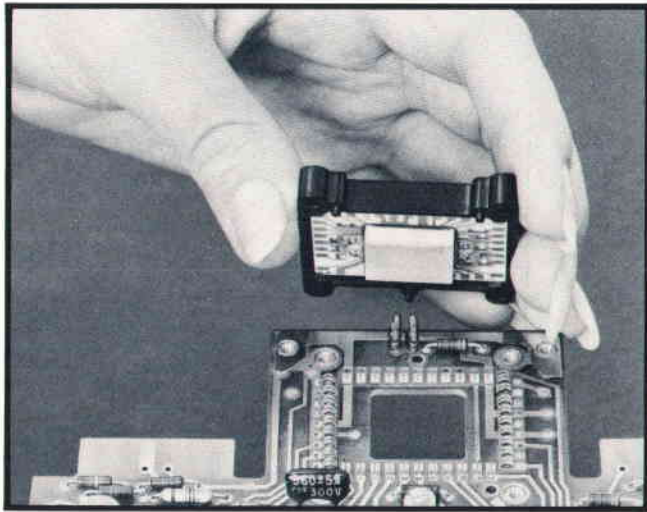


**Fig. 7.** Pre-amplifier hybrid IC makes electrical connection to the circuit board through spring contacts, simplifying removal and replacement.

familiar Miller integrator. The sweep trigger circuits, however, use a new circuit arrangement that does not have a tunnel-diode trigger recognizer, as was formerly required by wideband scopes.

A block diagram is shown in Fig. 8. The three Schmitt triggers function somewhat as OR gates, with the output going low only when both inputs are low. Operation is as follows.

With all circuits reset after the preceding sweep cycle, the output of the reset-control Schmitt is low, applying one low input to Schmitt A. When the input signal crosses below the threshold, the other input to Schmitt A goes low, causing one input to Schmitt B to go low. When the input signal brings the second input of Schmitt B below the threshold (one-half cycle

later with a sine wave), the output of Schmitt B goes low, starting a sweep. Because of the use of a differential signal input, it is not possible for Schmitts A and B to change states at the same time. Trigger ambiguities are thus prevented.

Once a sweep has started, the sync signal cannot reset either Schmitt A or B because of the Schmitt hysteresis, as shown by the waveforms in Fig. 8. The sweep continues until the sweep voltage rises to a level that triggers the reset circuit which in turn sets all of the Schmitt circuit outputs high, terminating the sweep.

The output of the reset ramp remains high until the holdoff circuit allows the first input to the reset control Schmitt to go low again, at which time the circuit becomes "armed", awaiting another trigger. The duration of the holdoff period is adjustable from the front panel, a convenience when a complicated waveform has more than one trigger point. The hold-off control allows the operator to delay the next trigger until the desired point on the waveform occurs.

The three Schmitt triggers, two stages of amplification, and a dc-controlled trigger polarity switch are all on one IC chip. Short lead lengths, circuit repeatability, reliability, and moderate cost along with good triggering performance are direct benefits of this design.

### Sync Conditioning

The sync conditioning circuit that precedes the trigger circuit uses a two-path scheme similar to that used in the vertical channel attenuator. While giving dc stability with high-frequency response to beyond 300 MHz, it also provides for the various coupling and filter modes inexpensively. A simplified circuit

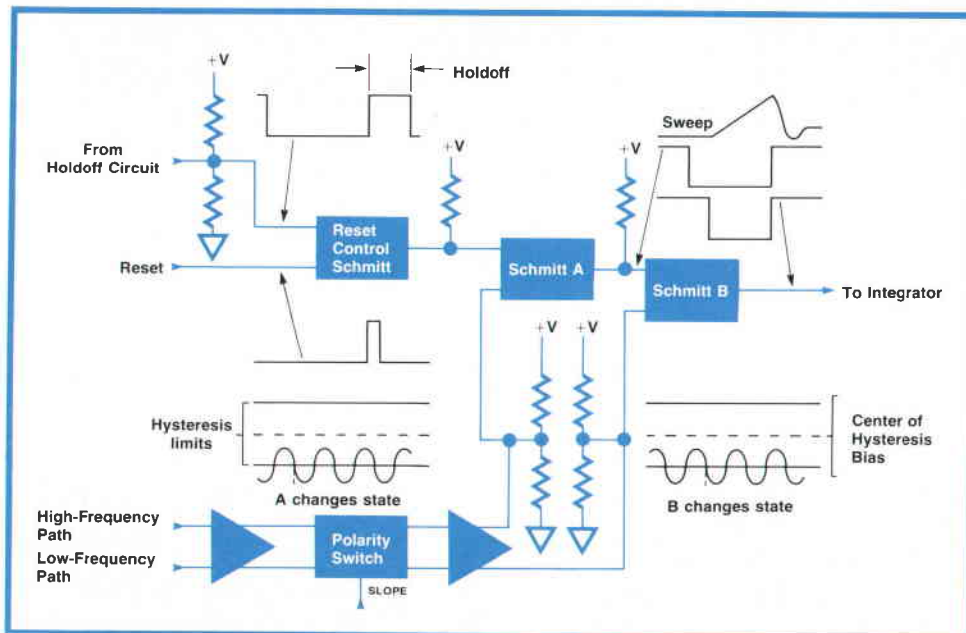


**Fig. 8.** Simplified diagram of the sweep trigger circuit. A sweep is started whenever the outputs of all three Schmitt trigger circuits are at a logic low. Hysteresis prevents the triggering waveform from resetting Schmitts A and B to the high state; that must be done by the reset waveform.

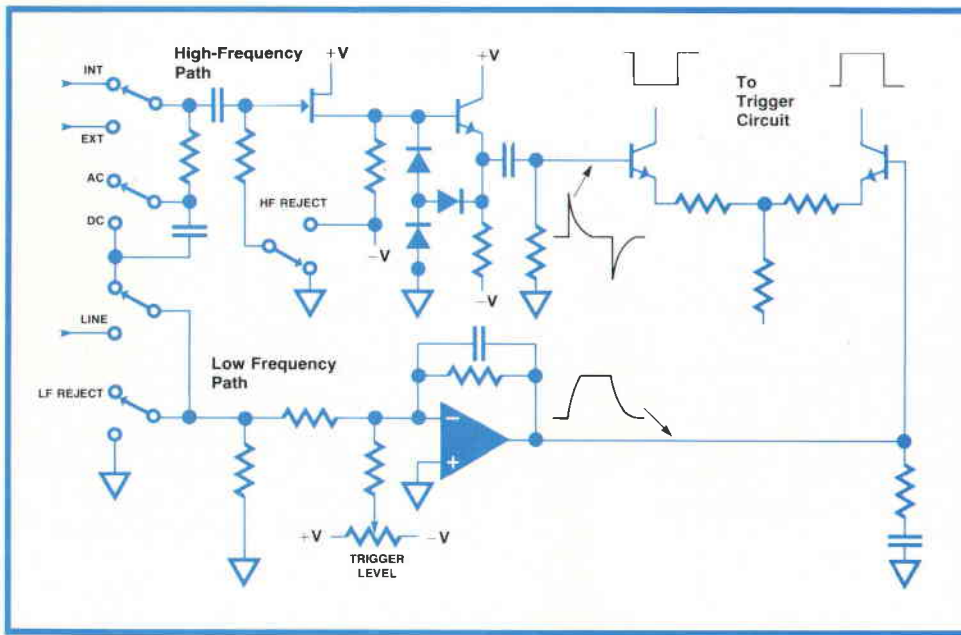


**Fig. 9.** Sync conditioning circuit uses a two-path scheme similar to the vertical attenuator. The outputs of the high- and low-frequency paths are summed by the differential amplifier (which is the first amplifier on the trigger IC chip).

diagram is shown in Fig. 9.

To use the high-frequency (HF) reject mode, the high frequency path is biased off. This mode is useful for preventing false triggering on noisy signals.

The low-frequency (LF) reject mode is effected by disconnecting the input to the low-frequency path. The circuit remains active, however, because it establishes the trigger level. This mode is useful for removing dc levels and low-frequency interference from the sync signal. The crossover frequency is 15 kHz.

Switching is arranged so that when the HF and LF REJECT pushbuttons are depressed at the same time, the sync circuit is transformer-coupled to the power line for syncing to the line frequency.

Because the two-path technique does not use passive filtering, it enables the instrument to have a high-impedance, low-capacitance external input (1 M $\Omega$ , 15 pF).

### Compensating Power Supplies

Since the new oscilloscope's circuits dissipate less than 100 W, it was decided to use conventional series-regulated power supplies rather than the more efficient switching regulator supply. This choice traded the switching regulator's noise and isolation problems for the series regulator's higher dissipation which, because of the instrument's relatively low power consumption, was easily accommodated by mounting the pass transistors on a rear-panel heat-sink.

Even though the supplies are stable with both time and temperature, they are interconnected to compensate for any changes in sweep timing accuracy that might result from minor changes in power supply voltage. All the power supplies are referenced to the

+15V supply and they track this voltage in proportion to the divider networks used. For example, a decrease in the +15V supply results in the same decrease in the -15V supply, which supplies the sweep circuit integrator current. The sweep would thus run slightly slower but in a time interval measurement, this would be offset by a decrease in delay time since the delay potentiometer is supplied from the +15V supply. This compensation is not 100% exact, because of component variations and calibration settings, but it is 90% effective—a 1% change in the +15V causes only a 0.1% change in a time-interval measurement.

The on-screen display is also compensated. The 1% decrease in the +15V supply causes a 1% decrease in the high-voltage supply, increasing deflection sensitivity to offset the decrease in sweep speed.

Another benefit of the design is that there is only one power supply calibration adjustment.

### Intensity Limit and Auto-focus

High-frequency oscilloscopes require a high intensity CRT spot to display fast moving, low-repetition rate waveforms. This capability could result in CRT damage with slower moving, high-repetition rate displays. The new Model 1720A reduces the possibility of such damage by using an intensity-limit circuit. This circuit senses the current in the first anode of the CRT and produces a voltage related to the average current. The voltage is used to reduce the height of the unblanking pulse as the average beam current increases, preventing the beam current from going too high. Note that for displaying hard-to-see low duty cycle signals, the average beam current is low so maximum available brightness is obtained.

An auto-focus circuit is included to reduce the need for readjusting the focus control as a variety of measurements are made. This circuit responds to the intensity control voltage, and modifies the focus voltage accordingly to maintain the beam in focus.

#### Acknowledgments

Bob Landgraf contributed to the vertical section. Horizontal CRT drive and the intensity control circuits were by John Poss. The CRT circuits and the power supplies were designed by Wayne Kohl and Jim Dolan and product design and packaging were carried out by Larry Gammill and Roger Molovar.

Rick James and Billy Ford contributed valuable technical support. The entire project team is deeply indebted to John Strathman for his support and encouragement during the early developmental stages, and to the HP Santa Clara Division for their efforts in the development and production of the integrated circuits. 

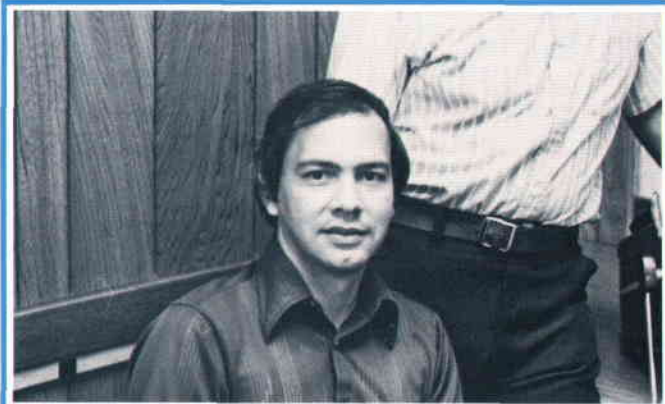
#### References

1. J. Pettit, "A DC-to-VHF Oscilloscope," Hewlett-Packard Journal, January 1970.
2. A.J. DeVilbiss, "A Wideband Oscilloscope Amplifier," Hewlett-Packard Journal, January 1970.



#### P. Kent Hardage

Kent Hardage obtained his BSEE from Texas Technological University in 1966, went to work in CRT production for HP, then returned to Texas Tech the following year with a teaching and research fellowship to earn his MSEE (1968). On returning to HP, he worked on the 183A Oscilloscope and plug-ins before assuming project leadership for the Model 1720A. He has now moved into LSI development. With three children at home (5, 4, and 1), he still finds time to do some cabinet-making and occasional fishing.



#### Thomas J. Zamborelli

Tom Zamborelli hails from Trinidad, Colorado. He earned his BSEE at Colorado State University in 1966 then went to work for HP as a production engineer. Three years later, he transferred to the engineering lab to work on 180-series plug-ins, along the way contributing a thick-film attenuator used in a number of HP's high-frequency scopes. He was responsible for the vertical channel in the 1720A. Tom has two boys 7 and 4 that join him on fishing expeditions but when its hunting season, he goes it alone.



#### S. Raymond Kushnir

A native of Pueblo, Colorado, Ray Kushnir earned his BSEE degree at the University of Colorado (1966) after which he went to work designing RF transmitters in the mid-west. A year and a half later, he joined HP and worked on a number of plug-ins for the 180-series oscilloscopes before getting involved in the 1720A time-base trigger circuit. In his spare time, he designs and builds hi-fi equipment. He's married but no family additions yet.

# SPECIFICATIONS

## Model 1720A Oscilloscope

### Vertical Display Modes

Channel A; channel B; channels A and B displayed alternately on successive sweeps (ALT), or by switching between channels at approx 1 MHz rate (CHOP); channel A plus channel B (algebraic addition).

### Vertical Amplifiers (2)

**BANDWIDTH** (3 dB down from a 6 div reference signal):  
DC-COUPLED: dc to 275 MHz in both 50 ohm and high impedance input modes.  
AC-COUPLED: Approx 10 Hz to 275 MHz.  
**RISE TIME:**  $\leq 1.3$  ns (measured from 10% to 90% points of 6 div input step).  
**BANDWIDTH LIMIT:** Limits upper bandwidth to approx 20 MHz.  
**DEFLECTION FACTOR**  
RANGES: 10 mV/div to 5 V/div in 1,2,5 sequence;  $\pm 2\%$  attenuator accuracy  
VERNIER: Continuously variable between all ranges, extends maximum deflection factor to at least 12.5 V/div.  
**POLARITY:** Channel B may be inverted by front-panel pushbutton.  
**SIGNAL DELAY:** Input signals are delayed sufficiently to view leading edge of input pulse without advanced trigger.  
**INPUT RC**  
AC and DC: 1 megohm  $\pm 2\%$  shunted by approx 11 pF.  
50 OHM: 50 ohms  $\pm 2\%$ ; VSWR,  $\leq 1.3:1$  on 10, 20, and 50 mV ranges and  $\leq 1.15:1$  on all other ranges.  
**TRIGGER SOURCE:** Selectable from channel A, channel B, or Composite.

### Vertical Output (Rear Panel)

**AMPLITUDE:** One division of vertical deflection produces approx 100 mV output (dc to 50 MHz).  
**CASCADED DEFLECTION FACTOR:** 1 mV/div with both vertical channels set to 10 mV/div.  
**CASCADED BANDWIDTH:** dc-5 MHz with bandwidth limit engaged.  
**VERTICAL OUTPUT SELECTION:** Trigger source set to channel A selects channel A output, trigger source set to channel B selects channel B output.

### Horizontal Display Modes

**SWEEP MODES:** Main, main intensified, mixed, and delayed.  
**SWEEP**  
RANGES: 10 ns/div to 0.5 s/div (24 ranges) 1,2,5 sequence.  
ACCURACY ( $0^\circ\text{C}$  to  $55^\circ\text{C}$ ):

MAIN SWEEP TIME/DIV	$\times 1$	$\times 10$
10 ns to 50 ns	$\pm 3\%$	$\pm 5\%$
100 ns to 20 ms	$\pm 2\%$	$\pm 3\%$
50 ms to 0.5 s	$\pm 3\%$	$\pm 3\%$

VERNIER: Continuously variable between all ranges, extends slowest sweep to at least 1.25 s/div.  
MAGNIFIER: Expands all sweeps by a factor of 10, extends fastest sweep to 1 ns/div.  
**SWEEP MODE**  
NORMAL: Sweep is triggered by internal or external signal.  
AUTOMATIC: Bright baseline displayed in absence of input signal. Triggering is same as normal above 40 Hz.  
SINGLE: In Normal mode, sweep occurs once with same triggering as normal; reset pushbutton arms sweep and lights indicator; in Auto mode, sweep occurs once each time Reset pushbutton is pressed.  
**TRIGGERING**  
INTERNAL: dc to 100 MHz on signals causing 0.5 division or more vertical deflection, increasing to 1 division of vertical deflection at 300 MHz in all display modes. Triggering on line frequency is also selectable.  
EXTERNAL: dc to 100 MHz on signals of 50 mV p-p or more increasing to 100 mV p-p at 300 MHz.  
EXTERNAL INPUT RC: Approx 1 megohm shunted by approx 15 pF.  
**TRIGGER LEVEL AND SLOPE**  
INTERNAL: At any point on vertical waveform displayed.  
EXTERNAL: Continuously variable from +1.0V to -1.0V on either slope of trigger signal, +10V to -10V in  $\div 10$  mode.  
**COUPLING:** AC, DC, LF REJ. or HF REJ.  
AC: Attenuates signals below approx 10 Hz.  
LF REJ: Attenuates signals below approx 15 kHz.  
HF REJ: Attenuates signals above approx 15 kHz.  
**TRIGGER HOLDOFF:** Time between sweeps continuously variable, exceeding one full sweep from 10 ns/div to 50 ms/div.

### Main Intensified

Intensifies that part of main time base to be expanded to full screen in delayed time base mode. Delay control adjusts position of intensified portion of sweep.

### Delayed Time Base

**SWEEP**  
RANGES: 10 ns/div to 20 ms/div (20 ranges) in 1,2,5 sequence.  
ACCURACY: Same as main time base.  
MAGNIFIER: Same as main time base.  
**TRIGGERING:**  
INTERNAL: Same as main time base except no Line Frequency triggering.  
STARTS AFTER DELAY: Delayed sweep automatically starts at end of delay.  
TRIGGER: With delayed trigger level control out of detent (Starts After Delay) delayed sweep is triggerable at end of delay period.  
EXTERNAL: Same as main time base.  
EXTERNAL INPUT RC: Approx 1 megohm shunted by approx 15 pF.  
**TRIGGER LEVEL AND SLOPE:** Same as main time base.  
**DELAY TIME:** Continuously variable from 10 ns to 5 sec.  
**DIFFERENTIAL TIME MEASUREMENT ACCURACY** ( $+15^\circ\text{C}$  to  $+35^\circ\text{C}$ ):

Main time base setting	Accuracy
50 ns/div to 20 ms/div	$\pm (0.5\% + 0.1\% \text{ of full scale})$
20ns/div and 50 ms/div to 0.5 s/div	$\pm (1\% + 0.2\% \text{ of full scale})$

**DELAY JITTER:**  $< 0.005\%$  (1 part in 20,000) of maximum delay in each step.

### Mixed Time Base

Dual time base in which main time base drives first portion of sweep and delayed time base completes sweep at faster rate.

### X-Y Operation

**BANDWIDTH**  
Y-AXIS (CHANNEL A): Same as channel A.  
X-AXIS (CHANNEL B): dc to  $> 3$  MHz.  
**PHASE DIFFERENCE BETWEEN CHANNELS:**  $< 3^\circ$ , dc to 3MHz.

### Cathode-Ray Tube and Controls

**TYPE:** Post accelerator, approx 20.5 kV accelerating potential, aluminumized P31 phosphor.  
**GRATICULE:**  $6 \times 10$  div internal graticule 0.2 subdivision markings on major horizontal and vertical axes 1 div = 1 cm. Internal flood gun graticule illumination.  
**BEAM FINDER:** Returns trace to CRT screen regardless of setting of horizontal, vertical, or intensity controls.  
**INTENSITY MODULATION:**  $\pm 8\text{V}$ ,  $\geq 50$  ns width pulse blanks trace of any intensity, useable to 20 MHz for normal intensity. Input R, 1 kohm  $\pm 10\%$ .  
**AUTO-FOCUS:** Automatically maintains beam focus with variations of intensity.  
**INTENSITY LIMIT:** Automatically limits beam current to decrease possible CRT damage.  
**REAR PANEL CONTROLS:** Astigmatism, pattern, main/delayed intensity ratio, and trace align.

### General

**REAR PANEL OUTPUTS:** Main and delayed gates.  $-0.7\text{V}$  to  $+1.3\text{V}$  capable of supplying approx 3 mA.  
**CALIBRATOR:**  
TYPE: 1 kHz  $\pm 10\%$  square wave.  
VOLTAGE: 3V p-p  $\pm 1\%$ .  
RISE TIME:  $< 0.1 \mu\text{s}$ .  
**POWER:** 100, 120, 220, 240,  $-10\%$   $+5\%$ , 48 to 440 Hz, 110 VA max.  
**WEIGHT:** Net, 28.5 lb (12.9 kg).  
**OPERATING ENVIRONMENT**  
TEMPERATURE:  $0^\circ\text{C}$  to  $55^\circ\text{C}$ .  
HUMIDITY: Up to 95% relative humidity at  $40^\circ\text{C}$ .  
ALTITUDE: To 15,000 ft (4.6 km).  
VIBRATION: Vibrated in three planes for 15 minutes each with 0.010 inch (0.0254 cm) excursion, 10 to 55 Hz.  
**DIMENSIONS:** 13-3/16 in W  $\times$  7-3/4 in H  $\times$  20 in D. (335  $\times$  197  $\times$  508 mm).  
**PRICE IN U.S.A.:** \$3400.  
**MANUFACTURING DIVISION:** COLORADO SPRINGS DIVISION  
Garden of the Gods Road  
Colorado Springs, Colorado 80907

# A Thin-Film/Semiconductor Thermocouple for Microwave Power Measurements

*This device is what makes it possible for the 435A/8481A Power Meter to outperform thin-film and thermistor power meters.*

by Weldon H. Jackson

ALTHOUGH THIN-FILM THERMOCOUPLES have been used for power measurements, they have suffered from low burnout levels and parasitic reactances that limited their frequency range. Semiconductors have been used primarily for thermoelectric cooling and have not been tried as power sensors. The thermocouple device used in the 8481A Power Sensor (see article, page 19) combines thin-film and semiconductor technology with an unusual structure to overcome previous limitations and gain several advantages.

The device, shown in Fig. 1, consists of two thermocouples on a single integrated-circuit chip. The main mass of material is silicon. The principal structural element is the frame of p-type silicon, which supports a thin web of n-type silicon. The smoothly sloped sides of the frame result from an anisotropic etch acting on the silicon crystal planes. The thin web is produced by epitaxially growing it on the p-type substrate and then suitably controlling the etch, which also reveals the surface of the diffused regions in the web.

Fig. 2 is a cross section through one of the thermocouples. The gold beam lead terminal penetrates the insulating silicon oxide surface layer to contact the web over the edge of the frame. This portion of the web has been more heavily doped by diffusing impurities into it. The connection between the gold lead and the diffused region is the cold junction of the thermocouple, and the diffused region is one leg of the thermocouple.

At the end of the diffused region near the center of the web, a second metal penetration to the web is made by a tantalum nitride film. This contact is the hot junction of the thermocouple. The tantalum nitride, which is deposited on the silicon oxide surface, continues to the edge of the frame, where it contacts the opposite beam lead terminal. The tantalum

nitride forms the other leg of the thermocouple.

The thermocouple is self-heated: microwave power dissipated in the tantalum nitride resistive film

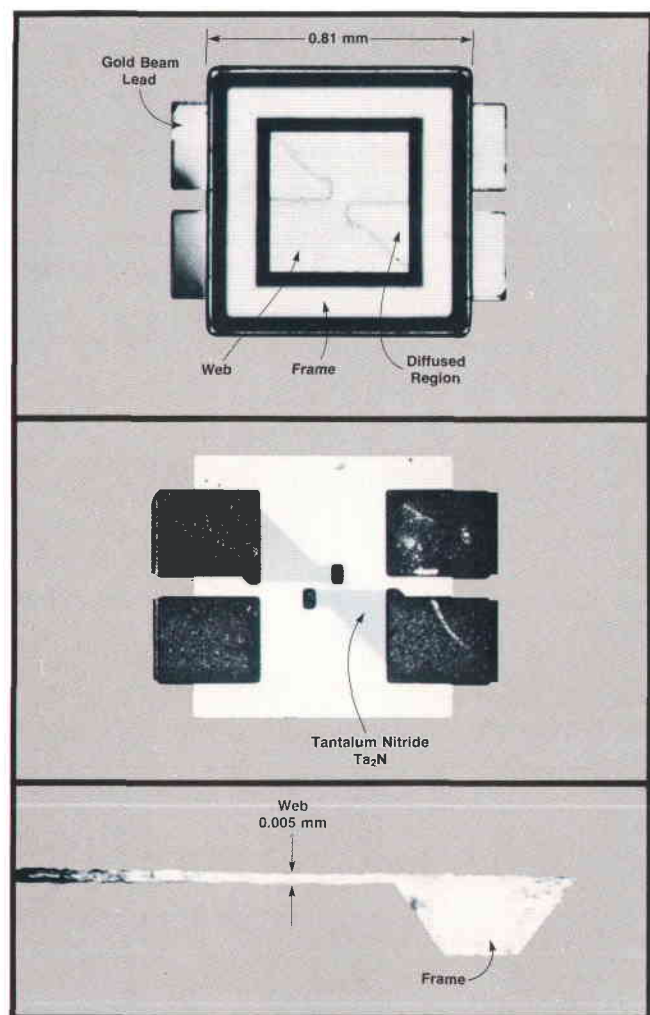
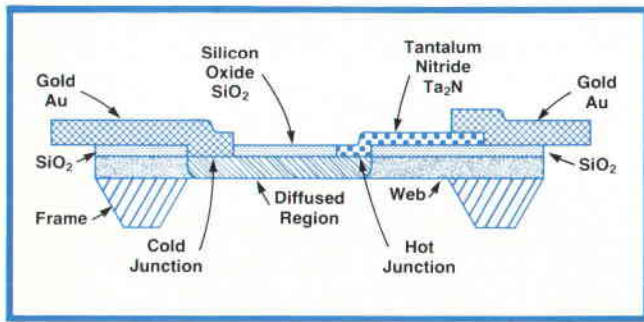


Fig. 1. Thermocouple chip consists of a silicon frame supporting a thin silicon web. Chip contains two thermocouples.



**Fig. 2.** Cross section of one thermocouple. The diffused region in the web is one leg of the thermocouple and the tantalum nitride film is the other. Power dissipated in the  $Ta_2N$  heats the hot junction.

generates the heat to raise the temperature of the hot junction above that of the cold junction, thereby producing a dc voltage across the thermocouple. The temperature rise and the dc voltage are proportional to the power dissipated, which is equal to the power of the source being measured if the thermocouple impedance is suitably matched to the source impedance (see article, page 19).

The thin web is very important, because the thermocouple output is proportional to the temperature difference between the hot and cold junctions. Silicon is quite a good thermal conductor, so it must be very thin if reasonable temperature differences are to be obtained from low power inputs.

### Device Design

Sensitivity in microvolts per milliwatt, which is proportional to thermoelectric power measured in microvolts per degree of temperature difference between the hot and cold junctions, is the fundamental parameter used to characterize thermocouple performance. For n-type silicon the thermoelectric power  $\alpha$  is:<sup>1</sup>

$$\alpha = 86.3 \left[ 2 + \ln \frac{2.5 \times 10^{19}}{n} + \frac{3}{2} \ln \frac{T}{300} \right] \mu V/^{\circ}C$$

where  $n$  = electron (donor) concentration ( $cm^{-3}$ )

$T$  = absolute temperature (K).

This equation tells us we can design the value of the thermoelectric power by properly choosing the electron concentration and that we will have to consider the effect of variations in thermoelectric power with temperature. Also, as is well known by semiconductor designers, the electron concentration determines the resistivity of the silicon, so a compromise must be made to achieve as much sensitivity as possible while minimizing the resistance.

The equation above is for a uniformly doped (uniform electron concentration) semiconductor. When dopants are added by diffusion, there is a very high concentration at the surface and the doping level

drops off rapidly with distance into the semiconductor. Since a description of the thermoelectric behavior of such nonuniform elements did not seem to exist in the literature, calculations were made using an approximate model consisting of ten uniform layers of different concentrations. The results compared well with measurements made on diffused silicon, as shown in Fig. 3.

The design value of the thermoelectric power was  $250 \mu V/^{\circ}C$ . The web thickness was selected so the hot-junction temperature rise was  $0.4^{\circ}C/mW$ . This results in a single-element sensitivity of  $100 \mu V/mW$ . In the complete structure, there is thermal coupling between the two elements and the sensitivity of the two-element device is  $160 \mu V/mW$ .

### Thermal Properties

Several interesting properties of the device follow from the choices made. The first is that the chosen linear dimensions of the web provide a thermal time constant of 120 microseconds. This means that the output of the device will fall exponentially to 37% of its initial value in 120 microseconds after steady-state power is removed.

Second, a reasonable estimate of the device destruction temperature is easily obtained. The device is known to break physically when driven with about 1.25 watts. At  $0.4^{\circ}C/mW$ , this corresponds to a hot-junction temperature rise of  $500^{\circ}C$ , which would produce a very large temperature gradient between the hot spot and thermal ground and could reasonably be expected to cause fracture. A check on this estimate is obtained by applying a slightly lower power of 1.125 watts and observing the rate of change of the tantalum nitride resistance (this rate is a known function of temperature). The observed rate of change is consistent with the  $500^{\circ}C$  estimate.

### Temperature Coefficient

As mentioned above, a temperature coefficient of sensitivity is to be expected. Fig. 4 shows the be-

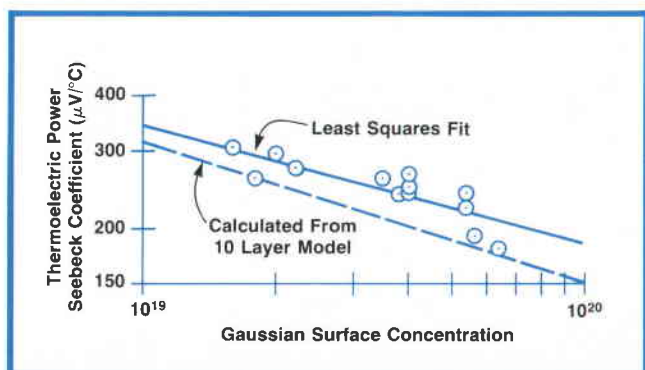


**Fig. 3.** Ten-layer model was used to predict thermocouple behavior. Calculations based on model agree well with measured values.

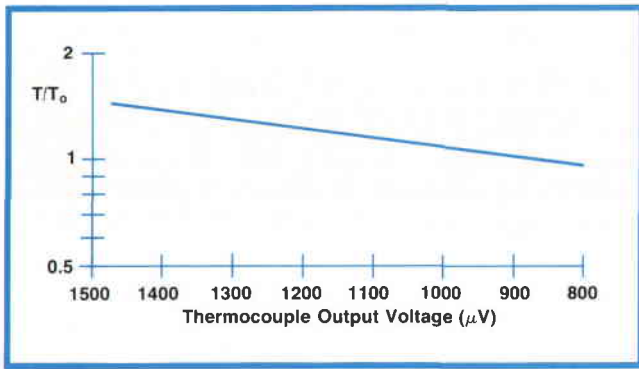


Fig. 4. Typical thermocouple sensitivity variation with temperature. Power level = 10mW,  $T_o$  = room temperature.

havior of a single thermocouple element, demonstrating that the thermocouple output is proportional to  $\ln(T/T_o)$ , where  $T_o=300K$ , as predicted by the thermoelectric power equation.

This temperature dependence makes the device response slightly nonlinear. However, the non-linearity is significant only on the highest ranges. The output at high power levels is slightly higher than that predicted by linear extrapolation from low power levels. At 30 mW the deviation is about 3% and at 100 mW it is about 10%. This is caused by the rise in the thermocouple average temperature, a substantial part of which is a rise in the cold junction temperature. Compensation circuitry in the 435A Power Meter eliminates the effect of this nonlinearity.

Increases in ambient temperature produce a similar effect. Circuitry in the 8481A Power Sensor compensates for this effect.

Another temperature-related variable is the temperature coefficient of resistance, which is about 350 ppm/°C for the whole structure. In the worst

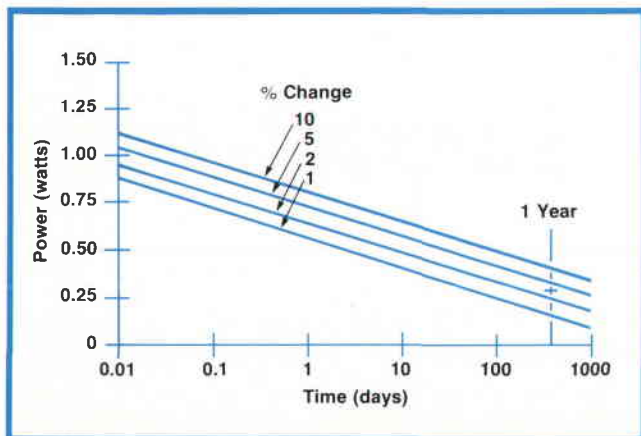


Fig. 5. Results of step stress aging test show percent change in thermocouple resistance when left at various power levels continuously for various periods of time. One year at 300 mW causes only a 3.5% change.

case, with a 55°C ambient temperature and maximum power, the average temperature rise is 20°C, and the resistance of the unit increases by only 2.6%. This has negligible effect on the standing-wave ratio of the sensor.

### Aging Effects

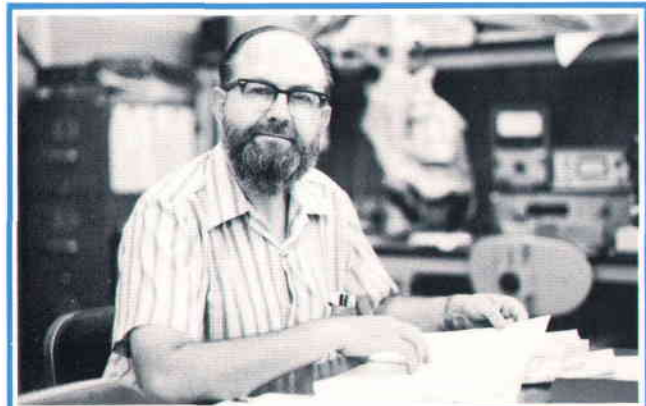
The only aging mechanism found so far is the resistance change caused by thermal aging of the tantalum nitride. A step stress test was made on a set of devices, producing the results shown in Fig. 5. These curves predict that if the device is left at 300 mW continuously for one year the resistance should increase by about 3.5%. The increase is only 2% if left at 1/2 watt for nine days. Aging is accumulative.

### Acknowledgments

I especially want to thank Bob Gray for his contribution to the thermal characterization of the device, for process development and for bringing the device fabrication into production. Working closely with Bob were Sam Burriesci and Mary Bradshaw who persevered when results were in doubt.

### Reference

1. V.A. Johnson, "Theory of the Seebeck Effect in Semiconductors," Progress in Semiconductors, Heywood and Co. Ltd., 1956, p. 68.



### Weldon H. Jackson

Before joining HP in 1967, Weldon Jackson was a member of the technical staff of Bell Telephone Laboratories for thirteen years, working on development of passive components, field-effect devices, and thin-film technology. His HP projects have been in the field of thin-film and hybrid technology. He has co-authored several professional papers on thin-film and semiconductor circuits and holds three patents, one of which is on the thermocouple power sensor for the 435A/8481A Power Meter. Now a section manager in hybrid research and development, he is a member of IEEE, the American Vacuum Society, and the Electrochemical Society. Weldon served in the U.S. Navy from 1944 to 1946 and received his BSEE degree in 1954 from California Institute of Technology. He is married, has two grown children, and enjoys hiking and listening to music. The Jacksons live in Sunnyvale, California.

# Microelectronics Enhances Thermocouple Power Measurements

*Day-to-day microwave power measurement accuracy is substantially improved by this new thermocouple power meter system, without sacrificing the convenience of earlier thermistor instruments.*

by John C. Lamy

**T**HERMISTOR POWER SENSORS and balanced bridge techniques are currently the most widely used tools for microwave power measurements. In theory, this combination has high inherent accuracy, guaranteed by feedback-controlled power substitution. In practice, however, the system suffers from several drawbacks that reduce the accuracy and the dynamic range in typical applications. The main accuracy limitation has been the mismatch uncertainty caused by thermistor mount standing wave ratio (SWR), and dynamic range is compromised by a relatively low burnout level and by relatively high thermal drift, even in temperature-compensated mounts.

The new Model 435A/8481A Thermocouple Power Meter System, Fig. 1, uses a different approach that, enhanced by microelectronics technology, contributes significantly to the usable accuracy and dynamic range of the power measurement system. The approach is simple: microwave power is dissipated in the hot junction of a thermocouple, producing a low-level dc voltage proportional to the applied power. This voltage is amplified and connected to a meter movement. The system gain is calibrated such that the meter reads power. A major benefit of this approach is that each block is amenable to recent technological innovations that result in an overall system superior to those of the past.

The 435A/8481A Power Meter makes substantial improvements in the accuracy of day-to-day power measurements, while sacrificing none of the convenience offered by such thermistor instruments as the HP 432A/8478B. Accuracy improvements come from lower input SWR, lower drift, individual sensor calibration, and a built-in reference oscillator. Convenience features carried over from the 432A include an autozero circuit that allows the user to set his meter offset to zero simply by pushing a button, and op-

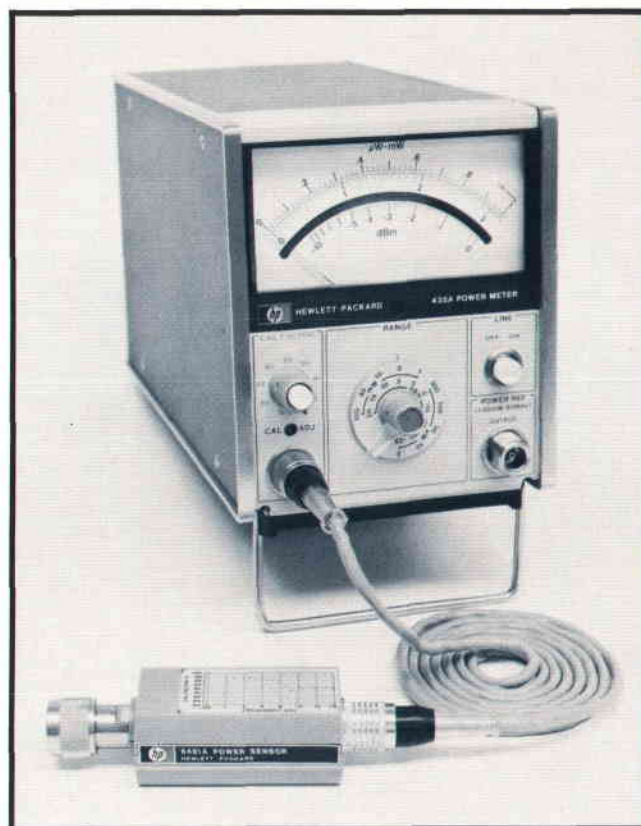


**Fig. 1.** Model 435A Power Meter with Model 8481A Thermocouple Power Sensor measures power from  $3\mu\text{W}$  to  $100\text{mW}$  and from 10 MHz to 18 GHz. Accuracy is substantially better than thermistor systems.

tional battery power.

The 8481A power sensor has 15 dB more dynamic range than thermistor mounts. It operates from 10 MHz to 18 GHz and from  $3\mu\text{W}$  to  $100\text{mW}$ . This makes it significantly more convenient than alternative systems that require several units to cover the same frequency or power range. Four other sensors extend

the system's frequency range down to 100 kHz and its power measurement range up to three watts.

### Mismatch Uncertainty

The largest single source of error in practical power measurements is the mismatch uncertainty. The typical uncertainty in X-band may be  $\pm 10\%$  or more. This uncertainty results from the interaction of source reflections and power sensor reflections, and is unwieldy to compensate because compensation requires knowing the magnitudes and phases of both reflection coefficients.

The only practical way to improve accuracy is to reduce the power sensor reflection. The 8481A has significantly lower reflection coefficient than other power meter mounts ( $|\Gamma| = 0.123$  at 18 GHz versus  $|\Gamma| = 0.230$  for the 8478B thermistor mount). Thus, for example, when measuring a source with  $SWR = 2$ , the limits of uncertainty are approximately  $\pm 9\%$ , compared with  $\pm 17\%$  for the 8478A. In addition, each 8481A is provided with a list of individually calibrated reflection coefficients at 17 frequencies. Thus the actual reflection may be used in place of the specified maximum; this usually provides a further reduction of uncertainty.

What makes this superior match performance possible is the extremely small size and high uniformity of the thermocouple device used in the 8481A sensor (see article, page 16). This device is a silicon chip 0.76 mm square. It has beam leads and contains two independent thermocouples, each of which is a 100-ohm resistor. The resistors are in parallel for incident microwave power, but in series for the dc output (see Fig. 2). Thus the dc can be taken from an RF ground point, namely the broadband bypass capacitor. Any other approach would require a broadband RF choke, which is more difficult to realize than a broadband bypass capacitor.

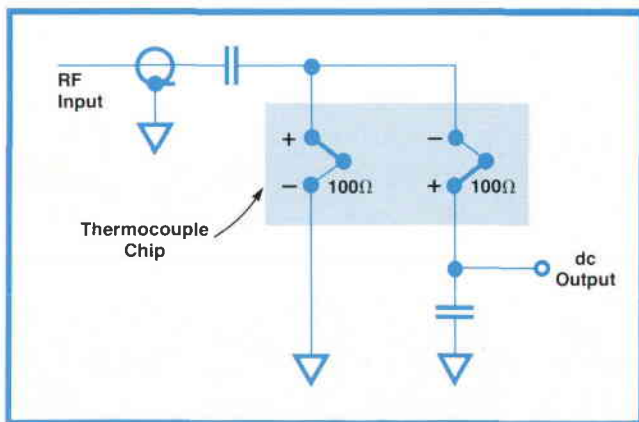


**Fig. 2.** Sensor contains two thermocouples, which are in parallel for incident microwave power but in series for the dc output. The thermocouple chip is fabricated using thin-film microelectronics technology. Its small size helps reduce temperature drift.

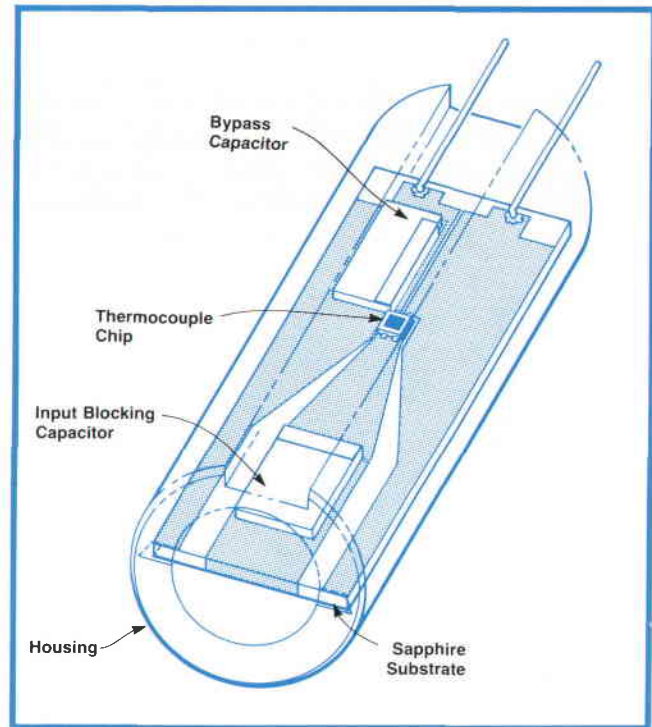


**Fig. 3.** Sensor RF structure also uses thin-film technology. Coplanar line on sapphire substrate has low parasitic inductance, essential for low reflection coefficient.

The sensor's RF structure is fabricated on a 0.63-mm-thick sapphire substrate, using thin-film microelectronics technology. Input RF power is carried on a tapered line with the ground in the same plane as the center conductor (coplanar line). The substrate is carried in a brass cylinder of 7-mm inside diameter, compatible with standard 7-mm connectors. The geometry and dimensions of the structure represent a trade-off: low reflection and freedom from unwanted modes require small size, but high-value capacitors for low-frequency performance require larger size. The dimensions finally chosen are a compromise between these two considerations (see Fig. 3).

Coplanar line is particularly attractive in this application because the ground plane can be brought arbitrarily close to the center conductor by a simple taper. This allows the thermocouple chip to be attached with a minimum of parasitic inductance. Low parasitics are essential to achieving a low reflection coefficient and therefore a low mismatch uncertainty.

### Calibration

A second contributor to high system accuracy is the individual calibration. Each 8481A power sensor is calibrated at seventeen frequencies for calibration factor, effective efficiency, and reflection coefficient magnitude and angle. Calibration is performed using an HP 8542B Automatic Network Analyzer with a special calibration test set, and an 8478B Thermistor

Mount certified by the U.S. National Bureau of Standards. The table below lists the worst-case uncertainties and rms (or probable) uncertainties in the calibration measurements.

Frequency (GHz)	Worst Case		Rms	
	Uncertainty (%)		Uncertainty (%)	
	Cal Factor	Effective Efficiency	Cal Factor	Effective Efficiency
4	2.65	2.65	1.55	1.55
12.4	2.35	2.25	1.40	1.34
18	5.25	4.75	3.22	2.91

Rms uncertainty is the square root of the sum of the individual uncertainties squared.

Individual calibration enhances accuracy in two ways. First, the actual calibration factor and effective efficiency are always known for a frequency very close ( $\pm 0.5$  GHz) to that of the measured signal. These numbers are displayed graphically on the side of the power sensor. Second, the sensor's actual reflection coefficient, not the specified maximum, may be used to compute the mismatch uncertainty. Since the typical sensor's performance at most frequencies is significantly better than specified, substantial reductions in mismatch uncertainty can be obtained this way. To make this feature convenient for the user, each sensor is shipped with a small printout of its calibration that can be kept with the sensor (Fig. 4).

SERIAL NUMBER 481.				
MHZ	EEZ	CF-2	RHO	ANG
2000	98.4	98.4	.020	-81.6
3000	98.1	98.1	.018	149.3
4000	98.0	97.9	.022	14.0
5000	97.8	97.8	.021	-95.8
6000	97.5	97.5	.010	125.2
7000	96.4	96.4	.019	-50.0
8000	95.8	95.7	.029	-169.7
9000	96.1	96.0	.040	67.9
10000	95.6	95.4	.051	-42.3
11000	95.2	95.1	.044	-141.7
12400	95.2	95.1	.035	43.8
13000	94.5	94.3	.045	-18.7
14000	94.4	94.1	.059	-93.0
15000	94.5	94.2	.053	-173.8
16000	93.8	93.7	.018	25.0
17000	94.5	94.0	.070	-115.6
17999	95.9	95.0	.095	150.2

Fig. 4. Each sensor is shipped with a small printout of its calibration at 17 frequencies. Calibration factors are also plotted on the side of each sensor.

### Reference Oscillator

A frequent, often well directed criticism of thermocouple power measurements is that such measurements are essentially open-loop, and that thermistor mounts, using power substitution, are inherently more accurate. The 435A/8481A system solves this problem and provides additional convenience and confidence at the same time. The 435A has an internal 50-MHz oscillator whose output power is controlled very accurately. If a user wishes to verify the accuracy of his system, he connects his sensor to the power reference output and, using a front-panel screwdriver adjustment, sets his 435A to read 1.00 mW. Confidence is assured because the RF is applied to the input port just like the measured RF. There is no dc-to-RF error or dual-element substitution error. The user has the added convenience of having a 50-MHz, 1.00-mW precision signal source in his power meter. This feature effectively transforms the system to a closed-loop measurement system.

The primary design considerations for the 50-MHz oscillator were long-term stability and temperature stability of its output amplitude. Harmonics had to be at least 30 dB down for 0.1% power ambiguity. Source SWR had to be under 1.04 to eliminate mismatch uncertainty considerations. Frequency accuracy is relatively unimportant since the sensor is very flat for moderate percentage frequency changes.

The circuit finally chosen is a leveled oscillator. Signal level is sensed by a peak detector, which introduces a small but acceptable amount of harmonic distortion. The detected signal is compared with a temperature-compensated reference, and the difference voltage controls the gain of the primary oscillator loop. Leveling takes place at a high signal voltage ( $\sim 10$  volts peak to peak), so millivolt-level temperature and aging effects are small by comparison. The high-voltage signal is divided down to the desired level by stable, temperature-tracking capacitors. Worst-case stability and rms stability of the power reference output are:

	Worst Case	Rms or Typical
Temperature Coefficient	0.02%/°C	0.0079%/°C
Aging	0.54%/Year	0.256%/Year

### Low-Level Performance

Users of microwave power meters have grown accustomed to the difficulty of making low-level power measurements. Zero drift caused by a warm hand or a warm instrument is the main culprit. The best thermistor mounts relieve this problem to a moderate degree by thermal balance techniques. But on low ranges, they still suffer from the fundamental issue, that balance results from subtracting two large quantities (power, in this case), so small errors in tempera-

ture tracking can produce large zero drift on the low ranges.

The 8481A sensor uses a different philosophy to achieve low temperature drift and, incidentally, immunity from other drift mechanisms. First, the thermal structure is inherently low-drift because it is small. To produce an indicated power output, a thermal gradient must exist across a part of the thermocouple that is 0.4 mm long. Also, this region is thermally short-circuited by the relatively massive sapphire substrate, and the entire structure is enclosed in a copper housing that further minimizes thermal gradients.

Drift considerations do not stop at the RF structure. The thermocouple dc output is very low-level (approximately 500 nV for 3 microwatts applied power), so it is difficult to transmit on an ordinary cable. Small, undesired thermocouples creep into the metal system at interfaces, hardness changes, points of wear and corrosion, and so on. This problem is multiplied if the user wants a 60-meter cable between his meter and sensor—a frequent request. For this reason it was decided to include the low-level dc circuitry in the power sensor, so only relatively high-level signals appear on the cable.

The only practical way to handle such low dc voltages is to “chop” them to a square wave, amplify this with an ac-coupled system, then synchronously detect the high level ac (see Fig. 5). For reasons mentioned above, it was decided to include the chopper

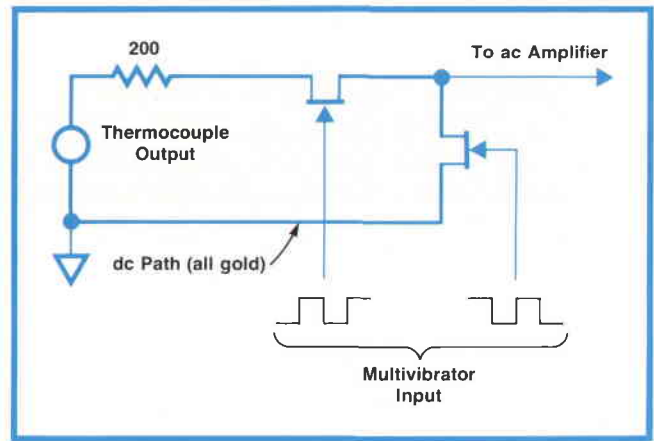


Fig. 6. Dc path in sensor is all gold to eliminate undesired thermocouples. Care was taken to assure that the two chopper FET's would remain at the same temperature to minimize drift.

and part of the first ac amplifier in the power sensor. The chopper itself (see Fig. 6) uses two discrete JFET's that are in intimate thermal contact with a beryllium oxide substrate. This was essential to keep the two FET's at exactly the same temperature, to minimize drift. To eliminate undesired thermocouples, care was taken to use only one metal, gold, throughout the entire dc path.

The net result of these efforts to eliminate drift is an order-of-magnitude improvement over the thermistor system. Fig. 7 shows a comparison of the two on the 10-microwatt range; the curves show the drift when

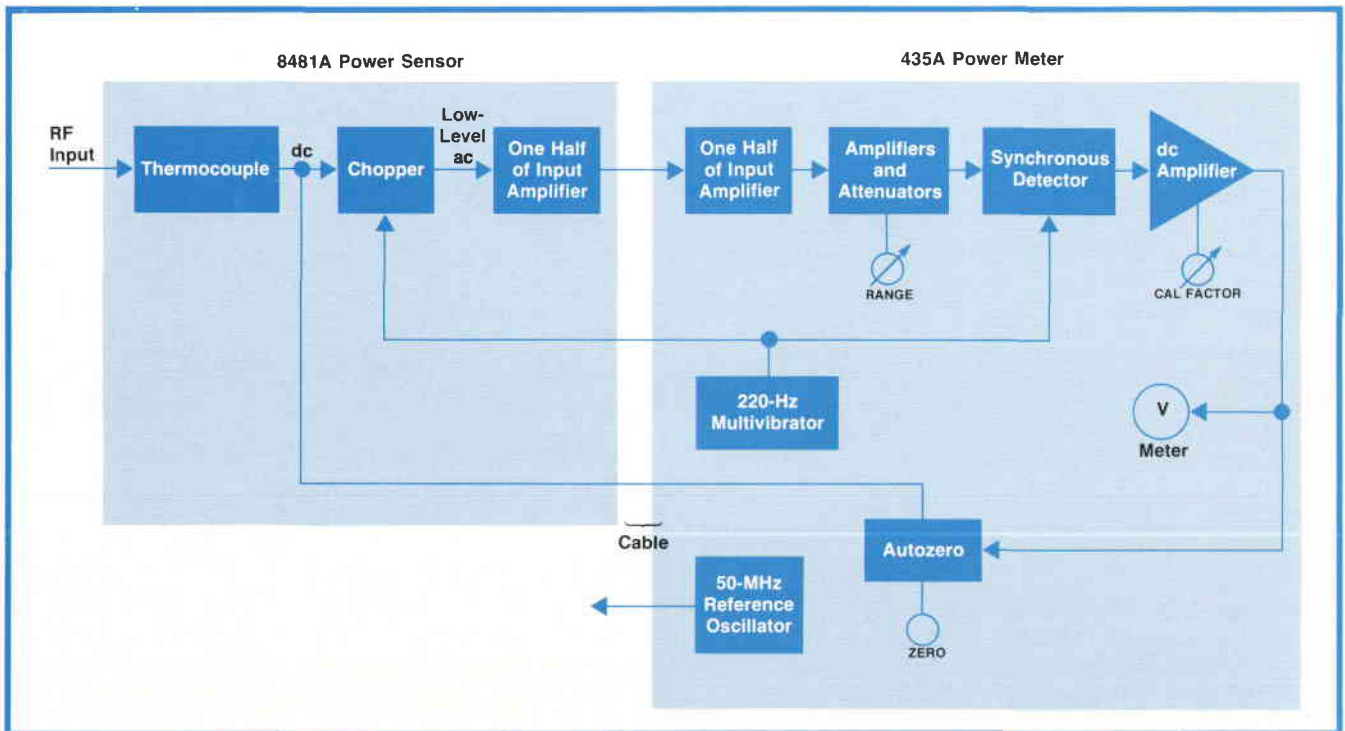


Fig. 5. 435A/8481A block diagram. 50-MHz reference oscillator provides a built-in accuracy check, effectively making the measurement system a closed-loop system.

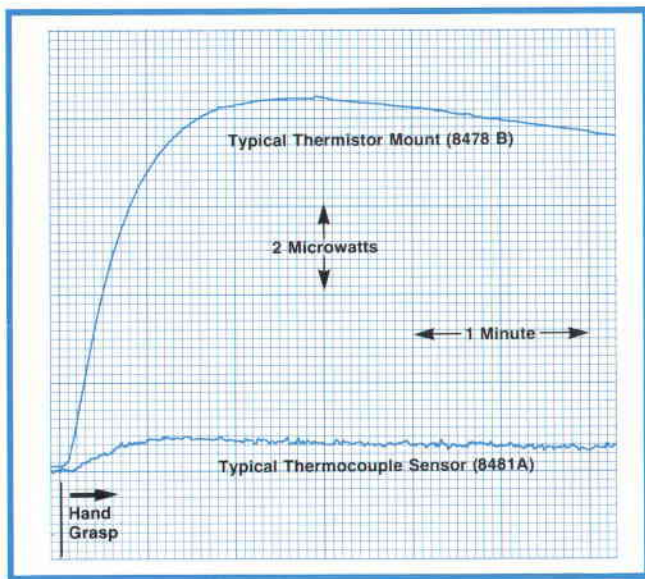


Fig. 7. Zero drift of thermocouple and thermistor power sensors after being grasped by a warm hand. Range is  $10\mu\text{W}$ .

the mount or sensor is firmly grasped by a hand—a typical annoying situation.

The 8481A and its cable are also more immune to physical shock and flexing than other systems. These advances allow the 435A/8481A system to have one more low-end range than thermistor systems:  $-25\text{ dBm}$ , rather than  $-20\text{ dBm}$ , is the low limit.

Performance factors that are sacrificed for these low-level improvements are noise and rise time on the low ranges. On the two lowest ranges, peak-to-peak noise is typically 2% of full scale. Rise time on the  $3\text{-}\mu\text{W}$  range is about two seconds, and on the  $10\text{-}\mu\text{W}$  range it is about 0.75 second. For most applications, these disadvantages are a small price to pay.

#### High-Level Performance

In most power meters the high end of the dynamic range is limited by the maximum power that can be applied without damaging the sensor. In typical thermistor mounts, blowout is specified at 30 milliwatts, so the highest usable range is 10 milliwatts. The thermocouple element used in the 8481A is substantially more rugged than typical thermistors or other thermocouples having equal sensitivity. This ruggedness results from the fabrication approach, a combination of thin-film and silicon technologies (see article, page 16). This makes possible a blowout specification of 300 milliwatts and a highest usable range of 100 milliwatts. The 300-milliwatt blowout specification is quite conservative; a typical sensor can withstand several days at  $\frac{1}{2}$  watt with negligible changes in sensitivity and resistance.

On the highest range the thermocouple output voltage becomes a slightly non-linear function of temperature. To correct for this effect, a nonlinear

compensation circuit is included in the first amplifier in the 435A Power Meter. The net error is well within the accuracy specification of the system.

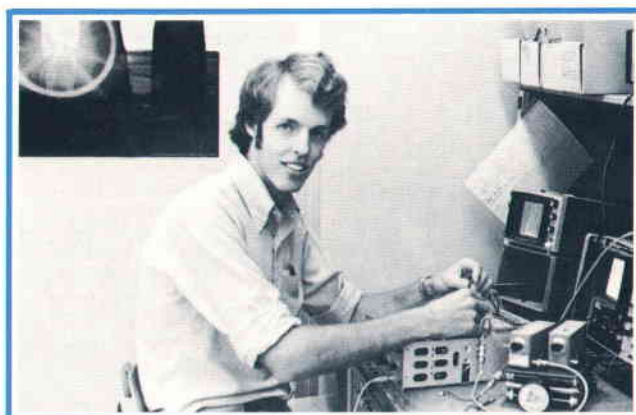
This same nonlinearity also tends to change the power reading as the ambient temperature changes. A temperature-dependent resistor in the 8481A Power Sensor compensates for this effect, cancelling it to well within the specification.

#### Other Sensors

Besides the basic Model 8481A sensor, four other sensors are available for the 435A Power Meter. Model 8482A is a 50-ohm sensor operating from 100 kHz to 4 GHz with SWR below 1.1 in the range 1 to 2000 MHz. Model 8483A is for 75-ohm systems, from 100 kHz to 2000 MHz; its SWR is 1.18 from 0.6 to 2000 MHz. Model 8481A Option H01 provides coverage from 10 MHz to 18 GHz over a dynamic range of 3 mW to 3 W, and Model 8482A Option H01 provides the same dynamic range from 100 kHz to 4 GHz.

#### Acknowledgments

Many people have contributed significantly to this project. Those I would especially like to thank are Weldon Jackson for supplying the thermocouple device that is the key component of the design, Bob Gray for the thermal design, Al Edwards for solutions to tough circuit design problems, Ron Trelle for product design, and Russ Riley for basic insights and contributions along the way. 



#### John C. Lamy

John Lamy was project leader for the 435A/8481A Power Meter. Born in Kansas City, Missouri, John graduated from Massachusetts Institute of Technology with a BSEE degree in 1968. He joined HP the same year and helped design the 8555A Spectrum Analyzer before taking on the power meter system. He holds one patent as a result of the 435A project. John is married and has a small son. He lives in Santa Rosa, California, where he and his wife spend much of their spare time working with the development of human potential in the Creative Initiative Foundation. Other activities include the Sonoma County Drug Abuse Council, photography, skiing, and backpacking.

## SPECIFICATIONS

### HP Model 435A Power Meter

**FREQUENCY RANGE:** 100 kHz to 18 GHz (depending on power sensor used).

**POWER RANGE:**

WITH 8481A, 8482A or 8483A SENSORS: 55 dB with 10 full-scale ranges of 3, 10, 30, 100 and 300  $\mu$ W; 1, 3, 10, 30, and 100 mW; also calibrated in dB from -25 dBm to +20 dBm full scale in 5 dB steps.

WITH 8481A-H01 or 8482A-H01 SENSORS: 50 dB with 9 full-scale ranges of 0.3, 1, 3, 10, 30, 100 and 300 mW; 1 and 3 W; also calibrated in dB from -5 dBm to +35 dBm full scale in 5 dB steps.

**INSTRUMENTATION UNCERTAINTY:**  $\pm 1\%$  of full scale on all ranges (0° to 55°C).

**ZERO CARRYOVER:**  $\pm 0.5\%$  of full scale when zeroed on the most sensitive range.

**REF OSC:** Internal oscillator with Type N female connector on front panel or rear panel (Option 003 only). Power output 1.00 mW  $\pm 0.70\%$  at 50 MHz (traceable to National Bureau of Standards).

**STABILITY:**  $\pm 0.2\%/^{\circ}\text{C}$  (0°-55°C).

**NOISE AND DRIFT (with 8481A, 8482A, and 8483A sensors):**  $< 1.5\%$  of full-scale-peak on 3  $\mu$ W range, less on higher ranges (typical, at constant temperature).

**RESPONSE TIME (with 8481A, 8482A, and 8483A sensors):** 2 seconds on 3  $\mu$ W range, 0.75 second on 10  $\mu$ W range, 0.25 second on 30  $\mu$ W range, and 100 msec on all other ranges. (Typical, time constant measured at recorder output.)

**ZERO:** Automatic, operated by front panel switch.

**CAL FACTOR:** 16-position switch normalizes meter reading to account for Calibration Factor or Effective Efficiency. Range 85% to 100% in 1% steps. 100% position corresponds to Calibration Factor at 50 MHz.

**RECORDER OUTPUT:** Proportional to indicated power with 1 volt corresponding to full scale; 1 k $\Omega$  output impedance, BNC connector.

**RF BLANKING OUTPUT:** Provides a contact closure to ground when auto-zero mode is engaged.

**CAL ADJ:** Front panel adjustment provides capability to adjust gain of meter to match power sensor in use.

**PRICES IN U.S.A.:**

435A Power Meter, \$700.00

8481A Power Sensor, \$360.00

Option 001: precision 7 mm (APC-7) connector, add \$25.00

Option H01: 0.3 mW to 3 W power range, add \$135.00

8482A RF Power Sensor, \$400.00

Option H01: 0.3 mW to 3 W power range, add \$135.00

8483A RF Power Sensor (75 $\Omega$ ), \$400.00.

**MANUFACTURING DIVISION:** STANFORD PARK DIVISION

1501 Page Mill Road

Palo Alto, California 94304

### Power Sensors

	8481A	8482A	8483A	8481A-H01*	8482A-H01*
Frequency Range:	10 MHz - 18 GHz	100 kHz - 4.2 GHz	100 kHz - 2 GHz	10 MHz - 18 GHz	100 kHz - 4.2 GHz
Nominal Impedance:	50 $\Omega$	50 $\Omega$	75 $\Omega$	50 $\Omega$	50 $\Omega$
Maximum SWR:	1.1	1.1	1.18	1.2	1.2
	50 MHz - 2 GHz	1 MHz - 2 GHz	600 kHz - 2 GHz	10 MHz - 8 GHz	100 kHz - 4.2 GHz
	1.18	1.2	1.8	1.3	
	30 - 50 MHz	300 kHz - 1 MHz	100 - 600 kHz	8 - 12.4 GHz	
	1.18	1.3		1.5	
	2 - 12.4 GHz	2 - 4.2 GHz		12.4 - 18 GHz	
	1.28	1.6			
	12.4 - 18 GHz	100 - 300 kHz			
	1.4				
	10 - 30 MHz				
Maximum Average Power:	300 mW	300 mW	300 mW	3.5 W	3.5 W
Maximum Peak Power:	15 W	15 W	10 W	100 W	100 W
Maximum Energy Per Pulse:	30 W- $\mu$ sec	30 W- $\mu$ sec	30 W- $\mu$ sec	100 W- $\mu$ sec	100 W- $\mu$ sec
Power Sensor Calibration:	Cal Factor data individually calibrated for each power sensor. The 8481A and 8481 A-H01 Sensors are also supplied with individual automatic network analyzer print out at 17 frequencies for Cal Factor and phase and magnitude of reflection.				

\* Only specifications listed in this table apply to H01 special options. No other specifications are implied.

Hewlett-Packard Company, 1501 Page Mill Road, Palo Alto, California 94304

Bulk Rate  
U.S. Postage  
Paid  
Hewlett-Packard  
Company

## HEWLETT-PACKARD JOURNAL

SEPTEMBER 1974 Volume 26 • Number 1

Technical Information from the Laboratories of  
Hewlett-Packard Company

Hewlett-Packard S.A., CH-1217 Meyrin 2  
Geneva, Switzerland

Yokogawa-Hewlett-Packard Ltd., Shibuya-Ku  
Tokyo 151 Japan

Editorial Director • Howard L. Roberts

Managing Editor • Richard P. Dolan

Art Director, Photographer • Arvid A. Danielson

Illustrator • Sue M. Perez

Administrative Services, Typography • Anne S. LoPresti

European Production Manager • Kurt Hungerbühler

**CHANGE OF ADDRESS** • To change your address or delete your name from our mailing list please send us your old address label (it peels off). Send changes to Hewlett-Packard Journal, 1501 Page Mill Road, Palo Alto, California 94304 U.S.A. Allow 60 days.

# HP Archive

This vintage Hewlett-Packard document was  
preserved and distributed by

**[www.hparchive.com](http://www.hparchive.com)**

Please visit us on the web!

On-line curator: John Miles, KE5FX

[jmiles@pop.net](mailto:jmiles@pop.net)

